A rapid, object-oriented approach to mapping and classifying wetlands at a regional scale in the central Congo River basin

Gregory William Bunker

Degree of Master of Science

Department of Geography

McGill University

Montreal, Quebec, Canada

January 25, 2010

A thesis submitted to McGill University in partial fulfillment of the requirements of the degree of Master of Science.

Acknowledgements

I would like to thank the Natural Sciences and Engineering Research Council (NSERC) of Canada, the Department of Geography at McGill University, the Global Environmental and Climate Change Centre (GEC^3), and my supervisor, Bernhard Lehner, for their financial support for this project. I would also like to thank Craig von Hagen for supplying the FAO Africover data, and my supervisor for supplying the JERS-1/SAR GRFM Africa and SWBD Lakes datasets. Also, many thanks to Raja Sengupta and Karina Benessaiah for lending the image analysis software. I would like to thank the members of my thesis advisory committee, Nigel Roulet and Margaret Kalacska, for their consultations, and Günther Grill and Elizabeth Heller for their technical support. Lastly, I am indebted to my supervisor for his patience, understanding and encouragement while I pursued this research. Completing this degree has presented many challenges and opportunities, and I was fortunate enough to benefit from a supervisor who made it all seem possible. For his ceaseless optimism and support, I am grateful.

Table of Contents

List of Tables

List of Figures

Abstract

Tropical floodplain wetlands are important from various perspectives, including hydrology, biogeochemistry and conservation, while facing imminent threats aggravated by insufficient baseline information. Recent advances in remote sensing and image analysis can address this problem. The integration of radar imagery (L-HH) with topographic datasets (elevation, slope and waterbodies) in an object-oriented analysis was tested as a method of rapid wetland mapping in the Equateur Province, Democratic Republic of Congo. Three classification schemes at different aggregation levels were produced to test thematic detail against accuracy. The highest level classifications include upland, lake, river, flooded forest, nonflooded forest, shrub and herbaceous vegetation. The maps range from 47% accuracy for the 7-class wetland map to 78% accuracy for the 3-class floodplain map compared to a reference map (FAO Africover). The method shows promise for developing inventories and monitoring programs to support wetland management in the central Congo River basin and other tropical riverine environments.

Abrégé

Les marécages tropicaux de zone inondable sont importants de diverses perspectives, incluant l'hydrologie, la biogéochimie et la conservation, tout en faisant face à des menaces imminentes aggravées par l'information insuffisante de ligne de base. Les avances récentes dans la télédétection et l'analyse d'image peuvent aborder ce problème. L'intégration des mosaïques de radar (L-HH) avec des ensembles de données topographiques (altitude, pente et cours d'eau) dans une analyse "object-oriented" a été examinée comme méthode de cartographie rapide pour les marécages dans la province d'Equateur, République Démocratique du Congo. Trois arrangements de classification à différents niveaux d'agrégation ont été produits pour examiner le détail thématique contre l'exactitude. Les classifications les plus detaillées incluent le terrain haute, le lac, le fleuve, la forêt inondée, la forêt non-inondée, l'arbuste et la végétation herbacée. Les cartes s'étendent de l'exactitude de 47% pour la carte de 7 classes à l'exactitude de 78% pour la carte de 3 classes comparée à une carte de référence (FAO Africover). La méthode se montre bien pour des inventaires et des programmes de surveillance qui soutiennent la gestion de marécage dans le bassin fluvial central du Congo et d'autres environnements riverains tropicaux.

1. Rationale, Objective, Research Questions and Literature Review

1.1 Rationale

The organic soils and proximity of wetland ecosystems to navigable water has led to their widespread conversion to agriculture and settlement. This traditional view of wetlands has caused between 26% and 50% of wetlands to be lost worldwide (Dugan 1993, Sterling and Ducharne 2008). Within the past 20 years, however, the global profile of wetlands has changed considerably because of their significance as modulators of climate and flooding and as habitat for many species and life stages of birds and fishes. Wetlands are now considered among the most valuable ecosystem types on Earth (Costanza et al. 1997). However, population and development pressures coupled with a lack of scientific information to ground policy virtually guarantees continued wetland loss (Davidson and Finlayson 2007).

Tropical floodplain wetlands face many imminent threats and challenges for management due to rapid population growth in combination with deforestation, agricultural expansion, and new hydropower projects (Junk 2002). Establishing policy to mitigate this loss is difficult because current wetland inventories and monitoring are not sufficient (Davidson and Finlayson 2007). Regional-scale tropical wetland inventories are absent or incomplete due to the lack of resources, indifferent political attitudes, and the difficult wetland terrain

generally found in tropical countries (Junk 2002). Inventories are the first step towards developing effective wetland policy and are essential for hydrology and biogeochemistry modeling, in addition to conservation planning. Although these motivations have led to wetland inventories of several Amazonian floodplain areas, these areas are in less danger of immediate loss or degradation than most other large tropical wetland areas (Junk 2002).

The Congo River basin is second only to the Amazon River basin in tropical wetland area, but will experience far greater demographic and development pressures than the Amazon by 2025 (Junk 2002). Although it is assumed that the majority of Congo wetlands remains intact (Campbell 2005), the population of the D. R. Congo (which comprises 60% of the basin area and the majority of Congo River wetlands) will more than double from 51 million people in 2000 to 115 million people in 2025 (United Nations 2000). At the same time, the vast natural resources of the country are being developed, which has motivated the planning of a massive hydropower project on the Congo River now undergoing a feasibility study (International Rivers 2008). These developments will affect the people who depend on the food (e.g., fish, rice) and building materials (e.g., reeds, clay) of the Congo wetlands, which cannot be readily substituted by the poor national or household economies of most countries in the basin (Coughanowr 1998). The physical functions of these wetlands (i.e., water

and carbon regulation, habitat structure) will also be affected but it is unclear how.

Although inventories have traditionally been collated from local knowledge, maps, reports, and aerial photography, these methods are time consuming and take years for large regions such as the Congo (e.g., White 1983). Recent advances in satellite remote sensing technology, image analysis and the growing availability of global and near-global, wetland-relevant, digital datasets provide standardized data that can be automatically classified, and show promise for developing rapid and repeatable large-scale wetland mapping methods (Houhoulis and Michener 2000, Mertes 2002).

1.2 Objective and Research Questions

The objective of this research is to develop a rapid, regional-scale method of tropical floodplain wetland classification without the use of field-based information based on the wetland-rich, 100,000 km^2 Equateur Province of the D. R. Congo in the central Congo River basin. The classification scheme is to be tailored to hydrologists, biogeochemists, and conservationists. Three important research questions follow from the trade-off between a “useful” and “rapid” classification method:

1. What tropical floodplain wetland classes are useful for hydrologists, biogeochemists, and conservationists?

2. What classes are achievable with reasonable effort and quality?

3. What is the best compromise between rapid analysis, thematic detail, and accuracy?

To familiarize the reader with this topic, previous work related to the satellite remote sensing of tropical floodplain wetlands at regional scales is described below.

1.3 Literature Review: Remote Sensing of Tropical Floodplain Wetlands

Floodplains are areas periodically inundated by the lateral overflow of rivers or lakes, and are extensive in the tropics because of the strong seasonal flooding of the low-gradient, well-weathered basins found there (Junk et al. 1989). These seasonal hydrologic pulses affect the development of floodplain geomorphology, soil, and vegetation depending on the amplitude, duration, and extent of flooding, and can be expressed as a gradient of physical and chemical conditions from the river proper to the surrounding uplands (Junk et al. 1989). This concept is known as the Aquatic-Terrestrial Transition Zone, or ATTZ, and it is the essential feature that maintains the diverse functions of tropical floodplain wetlands (Junk et al. 1989). The term “wetland” can be defined in many ways, but a common definition includes areas over which the water table is at or near the soil surface for a specified period of time during the year while also being vegetated (Sahagian and Melack 1998).

Tropical floodplain wetlands are interesting areas from several points of view. They are important as reserves for agriculture and settlement (Coughanowr 1998), as regulators of water and carbon and climate, (Chen and Prinn 2006, Lehner and Döll 2004), and as habitat for maintaining fisheries and biodiversity (Welcomme 1979, Hamilton et al. 2007). Mapping the seasonal extent of flooding and the distribution of wetland types is important for parameterizing hydrological and climate models (Lehner and Döll 2004); improving current and future carbon dioxide and methane emission estimates, processes and feedbacks (Richey et al. 2002, Melack et al. 2004); and for establishing and monitoring change of non-substitutable ecosystem services to humans and habitat to birds, fishes, and mammals (Coughanowr 1998, Thieme et al. 2007, Keddy et al. 2009). However, the large size, remoteness and dynamic nature of tropical floodplain wetlands have made them difficult to characterize with traditional methods of wetland classification.

Regional-scale vegetation maps exist for most of the tropics; however, they are based on traditional methods of landcover classification, which most often involves local knowledge, reports, and aerial photography (e.g., White 1983, Hughes et al. 1992). These methods are extremely time consuming and take years to compile for large regions (Ausseil et al. 2007). In most cases, tropical floodplain wetlands are not the focus of such landcover mapping efforts

and are reduced to a single class (e.g., White 1983). As these methods are not readily repeatable, they are not appropriate for monitoring the distribution, condition, and extent of tropical floodplain wetlands. Additionally, the many different sources of data used and the subjective nature of their interpretation cause wetland terminology to be ill-defined and inconsistent with classifications elsewhere (Lehner and Döll 2004). Regularly collected, standardized data and their objective analysis are required to inform policy development and large-scale questions of hydrology, biogeochemistry and conservation.

Satellite remote sensors are ideally suited to address this problem because they are able to make synoptic, regular observations for any given location on Earth. The convenience and consistency of applying satellite remote sensing to wetland mapping has led to nearly every type and size of wetland being studied this way (Ozesmi and Bauer 2002), especially large and remote floodplain environments (Mertes 2002). However, wetlands remain notoriously difficult to delineate and classify. Unlike other ecosystem types, wetlands are defined by water depth, seasonal extent, and water quality in addition to vegetation and soil types (Semeniuk and Semeniuk 1997). Characterizing wetland features has traditionally been constrained by limitations of information extraction from remotely sensed data (Mertes 2002), but the growing availability of global and near-global digital datasets and improvements in image

classification techniques show great potential to address these shortcomings (e.g., Hamilton et al. 2007, Durieux et al. 2007).

1.3.1 Optical Data

Most remote sensing approaches to wetland mapping involve one or two types of data: optical and (or) radar data. Optical sensors detect the relatively short wavelengths of solar radiation reflected from the Earth's surface, and are passive sensors because they rely on reflected solar radiation as the signal source. Optical data are most useful for detecting differences in leaf pigment concentrations between plant species (i.e., wavelengths in the visible spectrum), and detecting differences in leaf morphology and water content (i.e., wavelengths in the infrared spectrum). While spaceborne optical satellite systems (e.g., MODIS, LANDSAT, SPOT, IKONOS) are usually incapable of discriminating vegetation at the species level, their data are useful for mapping wetland vegetation communities, both emergent and submerged (Silva et al. 2008). The spectral signatures of emergent aquatic vegetation often overlap with terrestrial vegetation, water, and occasionally soil as well, which can affect visual interpretation of optical imagery (Ozesmi and Bauer 2002, Silva et al. 2008), but the use of a decision-tree classifier has been shown to improve wetland discrimination and accuracy (Baker et al. 2006). The reflectance of submerged aquatic vegetation is often very low and makes isolating the signal from water—

which absorbs most visible and infrared radiation—the primary challenge of identifying submerged vegetation (Silva et al. 2008). This step usually requires more sensitive techniques of atmospheric haze correction than the traditional Dark Object Subtraction method, which simply subtracts the value of open water (assuming it reflects zero radiation) from the spectral response of areas of interest elsewhere in the imagery (Silva et al. 2008). Although extensive vegetation information can be obtained from optical data, the inability to penetrate clouds and dense vegetation—a common phenomenon over wetlands, especially tropical ones—prevents optical data from becoming a reliable source of vegetation and flood extent data for large-scale inventory methods (Figure 1.1, De Grandi et al. 2000a, Hess et al. 2003, Rosenqvist et al. 2007).

1.3.2 Radar Data

Unlike the passive nature of optical sensors which depend on reflected solar energy, radar sensors are active, sending a pulse of radiation from the satellite to the target and then recording the amount reflected (Figure 1.1). The active nature and comparatively long (microwave) wavelength of radar signals mean that data can be collected independent of time of day or cloud cover. The most common radar bands used for tropical wetland mapping are C-band (5.6 cm) and L-band (23.5 cm) (De Grandi et al. 2000a, Costa et al. 2002, Mayaux et al. 2002, Hess et al. 2003, Hamilton et al. 2007, Durieux et al. 2007). Longer

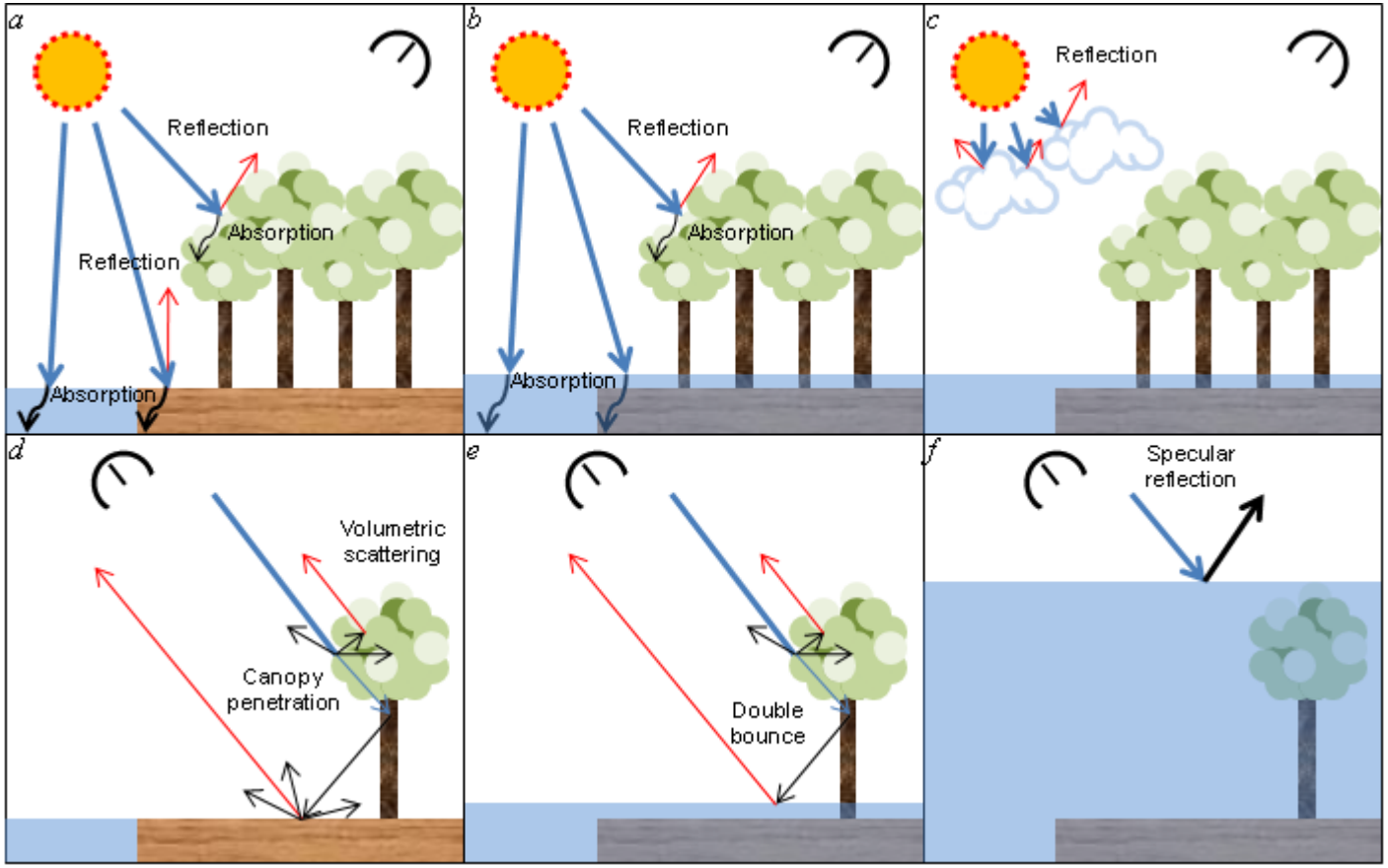

Figure 1.1: How optical (*a* to *c*) and radar (*d* to *f*) wavelengths interact with typical forested floodplain conditions. Blue arrows represent a source of electromagnetic energy, red arrows represent return signals to the sensor, black straight arrows represent signals reflected elsewhere, and black curved arrows represent absorbed energy. In diagrams (*d* to *f*), arrow thickness is proportionate to energy. Adapted from Rosenqvist et al. 2007.

wavelengths penetrate deeper into vegetation canopies, but lose sensitivity to smaller biophysical vegetation characteristics such as leaf distribution, density, orientation, canopy structure, and plant biomass (Silva et al. 2008). It is important to note that radar systems are side-looking, the inclination of which also affects the amount of energy that is returned as well as specularly reflected (Figure 1.1). Radar pulses can be returned to the sensor via the volumetric backscattering characteristic of vegetation canopies, and via the corner or di-hedral reflection characteristic of urban areas and flooded vegetation, where many surfaces occur at perpendicular angles (Figure 1.1). The longer wavelengths of radar data, compared to optical data, cannot penetrate water, so they are not sensitive to submerged vegetation, but can be sensitive to flooded vegetation stands.

C-band radar provides information about forest canopy structure via volume backscattering since it is often completely attenuated there (De Grandi et al. 2000, Mayaux et al. 2002), but also shows strong di-hedral reflectance from flooded herbaceous vegetation (Costa et al. 2002, Mayaux et al. 2002). The longer wavelength of L-band radar almost completely penetrates forest canopy vegetation and reflects a portion back to the sensor via corner-bouncing between the flooded surface and tree trunks (Silva et al. 2008). For this reason, L-band radar has long been used to reliably estimate the flood extent of flooded forest,

but is less successful at mapping wetland vegetation with less biomass such as shrub and herbaceous classes (e.g., Hess et al. 1995, Hess et al. 2003). However, radar data are increasingly considered a critical component of tropical wetland classifications due to their ability to penetrate cloud cover and their sensitivity to the presence of standing water beneath vegetation (Rosenqvist et al. 2007).

The latest generation of radar platforms provides an additional dimension of information with the ability to send and receive radar signals in different polarizations (e.g., RADARSAT-2, ALOS/PALSAR). Polarized electromagnetic radiation vibrates linearly. Traditionally, radar sensors have only recorded signals in same- or co-polarized wavelengths such as HH (sending and receiving a horizontally polarized wavelength, e.g., JERS-1/SAR) or VV (sending and receiving a vertically polarized wavelength, e.g., RADARSAT-1). The most advanced radar satellites now enable cross- (e.g., HV), dual- (e.g., HH+HV) and quad-polarization (HH+HV+VV+VH) techniques for much more complex vegetation structure analyses. Plant density, distribution, orientation, foliage shape, dielectric constant, canopy height, and soil moisture are all characteristics that radar still has the potential to capture in this way (Costa 2004). However, unlike optical spectral signatures, polarization signatures can be the same for two different scatterers (CCRS 2007).

1.3.3 Ancillary Data

Using only satellite imagery to classify tropical wetlands can be problematic (Sader et al. 1995). Tropical floodplain wetlands cannot necessarily be defined by their vegetation or flooding extent in a single satellite image, since wetland vegetation and flood extent are seasonally variable. Comparing or compositing multi-temporal imagery is one solution to this problem, but caveats remain. Coarse-resolution datasets provide regularity and homogeneity of acquisition dates at the expense of losing small features, which invariably includes most wetlands (Mayaux et al. 2004, Vancutsem et al. 2009). Fine-resolution datasets provide the necessary spatial and spectral detail to identify and classify wetlands, but suffer from the heterogeneity of acquisition dates and image availability (Vancutsem et al. 2009). Adding complimentary datasets can be a logical solution to the problem of temporally inconsistent imagery and rapid wetland mapping. Many wetlands are restricted to certain soils, slopes, and topography as well as to relationships with other landscape features that are not directly evident in satellite imagery (Sader et al. 1995). In this way, ancillary data add to the convergence of evidence needed for accurate wetland detection and classification (Sader et al. 1995).

Ancillary data are often added as a thematic layer in a Geographic Information System (GIS) for analysis, and typically improve wetland

classification provided that the data are co-registered accurately (Ozesmi and Bauer 2002). Common themes include soil types, elevation and other wetland maps (Ozesmi and Bauer 2002). In two of the earliest examples of multiple dataset analysis in a GIS, Bolstad and Lillesand (1992) and Sader et al. (1995) both found soil and elevation data aided in accurately classifying wetlands. Overall accuracy improved from 69% to 83% when soil texture and topographic position were considered. For floodplain wetland classification, Digital Elevation Models (DEMs) are particularly useful because they can readily highlight the low slope and elevation characteristics of floodplain geomorphology (Mertes 2002). Hamilton et al. (2006) combined the imagery from LANDSAT-7/ETM+ and JERS-1/SAR over a reach of the Madre de Dios River in the Peruvian Amazon with a DEM. The DEM was used in the initial step of their analysis to distinguish floodplain from nonfloodplain areas (Hamilton et al. 2007). This study employed a rule-based approach similar to Bolstad and Lillesand (1992) and Sader et al. (1995) which, being a knowledge-based method of analysis, is served well by ancillary data (Daniels 2006). Although ancillary data are useful for improving the accuracy and detail of wetland classification, ultimately it is the responsibility of the analyst to interpret and classify such data for practical use.

1.3.4 Image Analysis

Conceptually, pixel-based classification methods lack an intrinsic relationship to the boundaries of ecosystems since the boundaries of pixels are imposed during data processing (Hess et al. 2003). Pixel-based classification can also be problematic for ecological applications because the low statistical separability of classes results in either low accuracy or the use of very general classes (Lobo 1997). An object-oriented approach, in contrast, segments an image into more or less homogeneous regions (objects) that are then classified based on aggregate statistics of the pixels within the object.

Additionally, some software packages can semi-automatically, and thus rapidly, integrate several datasets of varying spatial and spectral resolutions into objects that can then be classified based on shape, texture, area, context, and information from other hierarchical object layers (e.g., Hamilton et al. 2007, Durieux et al. 2007). The object-oriented approach is proving to be an effective tool for improving the accuracy of and discriminating between wetland classes (Costa et al. 2002, Hess et al. 2003, Hamilton et al. 2007, Durieux et al. 2007). A distinct advantage of the object-oriented approach is that both descriptive and strategic information used for image segmentation and wetland classification are explicitly represented and changeable in the decision tree (or process tree),

allowing incremental improvement and new datasets and techniques to be added when applying or adapting a particular analysis elsewhere.

The concept of image segmentation as applied in an object-oriented approach is also very useful when analyzing radar data in particular. Radar data always include spurious data values known as speckle or noise. In a traditional pixel-based classifier these values would be classified differently from their neighbours despite the context of the situation (Oliver and Quegan 1998). An object-oriented approach builds objects from a single pixel and then, based on user-defined rules of homogeneity, grows and merges the single pixel with neighbours in an iterative process (Oliver and Quegan 1998). This technique alleviates the speckle issue of radar data and has been widely adopted for radar-based tropical wetland classification (Costa et al. 2002, Hess et al. 2003, Costa and Telmer 2007).

1.3.5 Tropical Floodplain Wetland Classification

For the purposes of large-scale hydrology and biogeochemistry research, especially for methane emissions, satellite radar imagery is sufficient for mapping functional wetland types. This is because hydrological models do not yet incorporate wetland functional vegetation classes, and because methane emissions from tropical wetlands are dependent on three basic floodplain environments with distinct differences in canopy structure (open water, emergent

herbaceous vegetation, and flooded forest) (Devol et al. 1990). Each of these environments involves different rates of water retention and evaporation, as well as production, oxidation and pathways of methane to the atmosphere. There remains considerable variability of methane release from each of these environments, but greater uncertainty lies in estimating the changing extent of these environments during the flooding cycles of tropical basins (Melack et al. 2004). The wetland classification scheme of Hess et al. (2003) successfully followed this approach and has since been used to improve the estimates of carbon dioxide degassing from the Amazon River (Richey et al. 2002) as well as to estimate the regional methane emissions from the Amazon basin (Melack et al. 2004).

Tropical floodplain wetland maps motivated by biodiversity and conservation concerns also benefit from a physiognomic-hydrologic classification scheme since such environments also provide information regarding fish habitat and fisheries management (Hess et al. 2003). The Ramsar Convention on Wetlands, an intergovernmental treaty meant to provide a framework for national and international cooperation towards the wise use and conservation of wetlands, also promotes remote sensing as a key tool for establishing national wetland inventories and monitoring programs to measure and achieve its goals (Rosenqvist et al. 2007). However, as radar data are generally incapable of

providing species-specific information, the addition of optical data provides more vegetation-based classifications that are necessary to distinguish important tropical wetland classes such as *Raphia* spp., for example (Hess et al. 2003, Hamilton et al. 2007). Wetland classification, regardless of thematic detail, must also include some measure of accuracy relative to ground conditions to be useful.

1.3.6 Accuracy Assessment

Map accuracy is the degree of correspondence between classification and reality on the ground (Congalton and Green 2009). It is determined by comparing the map of interest against other maps, imagery or, traditionally, observations in the field. The latter method is called ground-truthing, and it is the only true method of accuracy assessment for maps based on remotely sensed data. However, the time, finances and logistics of conducting field campaigns for large scale map verification—especially maps with a temporal element—can make it an impractical method of accuracy assessment (Mayaux et al. 2002). An effective alternative adopted in large-scale landcover studies in both the Amazon and Congo basins used videography combined with GPS during low-altitude flights across the area of interest as validation (De Grandi et al. 2000, Hess et al. 2003). This approach remains out of the financial realm of most map producers, however. Consequently, comparing one map to another map or type of imagery

is the most common method of large-scale assessments (De Grandi et al. 2000, Mayaux et al. 2002, Durieux et al. 2007, Congalton and Green 2009). There are several considerations with this approach: the timing of data collection for producing each map; the spatial resolution of each map; the minimum mapping areas of each class in each map; class definitions used in each map; and lastly, the positional and thematic accuracy of the reference map (Congalton and Green 2009). If these qualities do not match, or if the accuracy of the reference map is not acceptable, a quantitative assessment between the maps will not be useful, and a simpler qualitative, visual comparison between the maps must suffice (Congalton and Green 2009).

If these qualities match and if the accuracy of the reference map is acceptable, then a quantitative assessment can be performed. An error matrix (also known as a confusion matrix or contingency table) is the most common and useful method of comparing the level of correspondence between thematic maps (Congalton and Green 2009). An error matrix displays not only the number of mapping units (e.g., pixels, pixel groups, or polygons) from each class of the producer's map (in rows) correctly classified according to the classes of the reference map (in columns), but also how misclassified mapping units were classified instead (e.g., see Table 3.1). Therefore, an error matrix yields several measures of accuracy as explained below.

Overall accuracy is the sum of all correctly classified mapping units, regardless of class, divided by the total number of mapping units, and it is usually expressed as a percentage. There are no established thresholds for acceptable levels of overall accuracy: ultimately, what qualifies as acceptable is decided by the user. Large-scale tropical wetland studies show overall accuracies from approximately 75% with one to four classes to 95% with eight classes (see Case Studies in section 1.3.7 below).

Producer's accuracy is a measure of the accuracy of a particular classification scheme and shows what percentage of a particular reference class was correctly classified (CCRS 2009). Put another way, producer's accuracy is a measure of omission, excluding a mapping unit (pixel or object) from the category to which it truly belongs. Producer's accuracy is calculated by dividing the number of correct mapping units of a given class by the actual number of mapping units of that class in the reference map (CCRS 2009). Since producer's accuracy reflects the success of the producer to replicate a given class of the reference map, there could be an over-quantification error that could cause producer's accuracy to be high for a class. For example, in the field, it may be found that the given class, while mapped correctly according to the reference map, is overestimated at the expense of correct classifications elsewhere.

Providing user's accuracy helps to alert this possibility to the map user. User's accuracy is a measure of the reliability of an output map generated from a classification scheme, telling the user of the map what percentage of a class corresponds to the ground-truthed class (CCRS 2009). User's accuracy is a measure of classifying a mapping unit User's accuracy is calculated by dividing the number of correct mapping units of a given class by the total number of mapping units assigned to that class (CCRS 2009). It reflects the success of properly quantifying and locating the mapping units of a given class.

Another statistic widely used to determine the robustness of a classification is the Kappa Index of Agreement (KIA, also known as the Kappa or Khat statistic) (Congalton and Green 2009). It is given by subtracting the proportion of randomly, correctly classified mapping units (p_r) from the proportion of correctly classified mapping units (p_c), divided by the difference between 1 (a perfect classification) and the proportion of randomly, correctly classified mapping units (p_r) (i.e., $[(p_c) - (p_r)] / [1 - (p_r)]$). It can be interpreted as the proportion of correctly classified units beyond what could be explained by randomly labeling mapping units. Despite its wide use, the KIA confounds quantification and location error (Pontius Jr. 2000). It also does not penalize for large quantification errors or reward for accurate quantification (Pontius Jr. 2000).

Therefore, the KIA is not a perfect statistical descriptor and its weaknesses must be acknowledged in its interpretation.

Generally, it has been proposed that a KIA greater than 0.80 indicates strong agreement; a KIA between 0.40 and 0.80 indicates moderate agreement; and a KIA less than 0.40 indicates poor agreement (Landis and Koch 1977). However, when referring to and interpreting these thresholds one must also consider the quality of the reference data. Although no KIA has been reported in regional studies of the central Congo and Amazon basins, other means of accuracy have been employed to interpret the accuracy of these maps.

1.3.7 Case Studies: the Central Congo and Amazon River Basin Floodplains

The most studied wetlands of the Congo River basin lie in the *cuvette centrale congolaise*, its vast, well-weathered central floodplain. The wetlands of the central Congo basin were first mapped by White (1983) who took 15 years to compile national vegetation maps, consult local experts, and produce his continent-wide vegetation map based on physiognomy and floristics. White's swamp forest, the single wetland class of his exhaustive vegetation map of the continent, is composed of herbaceous swamp, aquatic vegetation, edaphic grassland, and riparian forest descriptions (White 1983). Although White's map is spatially simple, it contains considerable description of the swamp forest class.

However, this method is not appropriate for developing a consistent method of wetland inventories and updates needed for this rapidly developing region. The first satellite-produced vegetation maps of the region focused on establishing a baseline for forest cover in the basin. The spatial (1 km) and spectral resolution (4 bands visible, 2 bands infrared) of the optical composite imagery (NOAA/AVHRR) used in these studies was only able to distinguish between disturbed and undisturbed forest types, and overestimated forest cover by up to 20% due to the large spatial resolution (Laporte et al. 1995, Laporte et al. 1998, Mayaux et al. 1999a). Separating swamp forest from the tropical forest class with remotely sensed imagery was not possible until studies began to include radar imagery.

A single C-band radar dataset (ERS-1/SAR) of 100 m spatial resolution was used by De Grandi et al. (2000a) to distinguish lowland rain forest from swamp forest across the entire central basin, and Mayaux et al. (2000) incorporated the same dataset with optical datasets of larger resolution to make the same distinction in addition to other nonwetland classes. The C-band dataset enabled discrimination between lowland and swamp forest based on the texture, or variability, of the backscatter response over each type of canopy (Figure 1.2, De Grandi et al. 2000a, Mayaux et al. 2000). The difference in radar texture was verified using aerial videography, which showed that the lowland rain forest

canopy had considerably more variation in tree height, greater crown size, and more species, causing greater texture compared to the less diverse, flatter swamp forest canopy (De Grandi et al. 2000a). However, no underlying flooding could be detected with the C-band dataset since it was completely attenuated within the first 50 cm of the dense, closed lowland canopy (Mayaux et al. 2000). The overall accuracy of each map was determined by comparison to a D. R. Congo forest map derived from the visual interpretation of Landsat imagery corroborated with field and aerial surveys (SPIAF 1995). The map presented in De Grandi et al. (2000a) shows slightly lower overall accuracy at 71% compared to the multisensory approach of Mayaux et al. (2000), which found 75% overall accuracy. Most of the overall error was confusion between lowland rain forest and swamp forest.

To solve this, Mayaux et al. (2002) used a combination of C-VV (ERS-1/SAR) and L-HH (JERS-1/SAR) radar mosaics each taken from different time periods. There were several complications, however, when georegistering these radar data because of the different dates, resolutions, incident angles, and paths on which the data were collected. The analysis of these data was based on a rule-based hierarchical classifier. The rules were derived from training sets and visual inspection of local maps of the area of interest. From these data, eight classes were determined at 200 m resolution, three of which were wetlands:

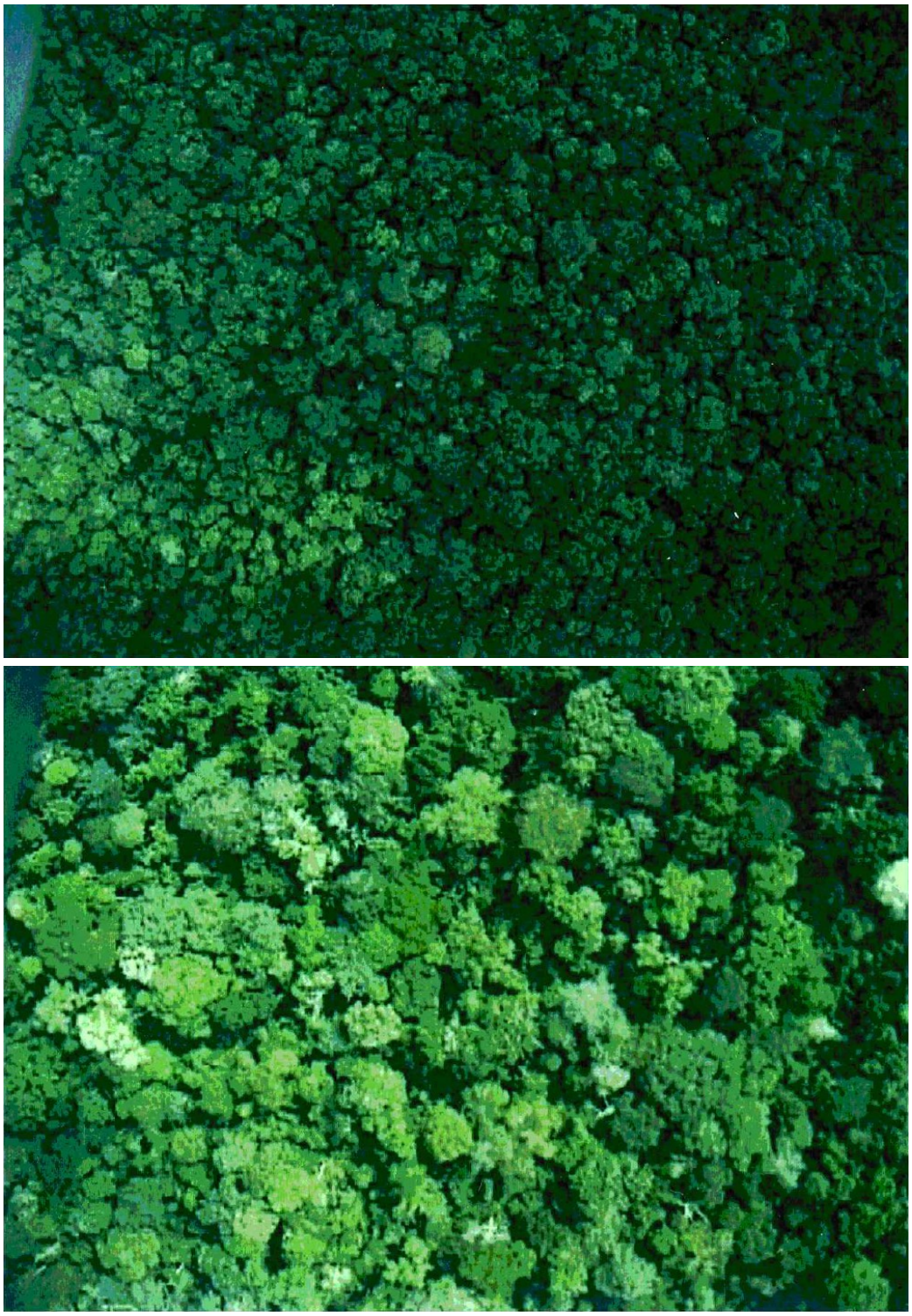

Figure 1.2: Aerial videography snapshots of swamp forest (above) and upland, or terra firme, forest (below) in the central Congo basin. From De Grandi et al. 2000a.

permanently flooded forest, periodically flooded forest, and swamp grassland. In addition to the added wetland class, the accuracy for this map was slightly higher than that of De Grandi et al. (2000a) and Mayaux et al. (2000) at 76% when compared to SPIAF (1995). Most of the error was the result of the enhanced wetland sensitivity of radar in comparison to the optical data used to produce SPIAF (1995), so 76% is likely an underestimate of the accuracy of the map. However, both the C-VV and L-HH data were unable to identify strips of secondary forest along river networks, whereas this forest type is easily discernable using optical imagery (Mayaux et al. 2002).

The most recent remote sensing of Congo vegetation used daily optical composites (SPOT/VGT) from the year 2000 at 1 km resolution to produce a new vegetation map of the D. R. Congo (Vancutsem et al. 2009). Of the six classes defined, two wetland classes were described: (1) edaphic forest and (2) aquatic grassland and swamp grassland. These classes constitute the smallest area of the landcover classes mapped. When experimenting with aggregated classes, Vancutsem et al. (2009) found that aquatic vegetation was responsible for most of the overall error with 56% underestimation compared to a reference map based on 30 m optical (LANDSAT) data (further detail regarding this dataset--Africover--is given in Methods below). Most of this inaccuracy was the result of the large resolution of the composites compared to the high resolution of the

reference map, which was able to identify typically small and linear wetland features (Vancutsem et al. 2009). This result of underestimating wetlands is similar to that found in Mayaux et al. (2004), which also used 1 km optical composites (NOAA/AVHRR). Finer spatial resolution than 1 km is necessary, therefore, to accurately determine wetland quantities for regional tropical floodplain wetlands. A study that addresses the issue of temporal and spatial resolution with an explicit focus on tropical floodplain wetlands comes from a study of the central Amazon.

Hess et al. (2003) provide an exemplary application of radar imagery for classifying tropical floodplain wetlands at a regional scale. Hess et al. (2003) were able to distinguish between wetland and nonwetland classes over the central basin of the Amazon River with 95% accuracy using two L-HH mosaics at 100 m resolution taken at high- and low-water conditions in the basin. The classification scheme was designed to improve regional hydrologic parameters (Sahagian and Melack 1998), carbon dioxide and methane emission estimates (Richey et al. 2002, Rosenqvist et al. 2002a), as well as fishery management, since many fish species depend on the flooded forests for nutrition or organic matter from floodplain algae (Forsberg et al. 1993). The eight wetland classes mapped include water, nonflooded bare or herbaceous, flooded herbaceous, nonflooded shrub, flooded shrub, flooded woodland, nonflooded forest, and

flooded forest. It was concluded that although L-HH is the best single-band sensor for mapping wetlands in the central Amazon basin, the backscatter from the most common nonwetland cover (nonflooded forest) overlaps with forest and aquatic macrophyte cover and serves as a major source of confusion for traditional, pixel-based classification methods.

These studies illustrate that coarse-resolution (> 1 km) though frequently collected optical imagery alone is not capable of reliably determining flooded vegetation classes, and suggest radar imagery as a primary source of flooded vegetation extent in tropical floodplain environments.

2. Approach, Study Area and Methods

2.1 Approach

Previous work demonstrates that radar imagery is useful for mapping several kinds of flooded vegetation in the tropics (De Grandi et al. 2000a, Mayaux et al. 2002, Hess et al. 2003, Rosenqvist et al. 2007). Indeed, Hess et al. (2003) was remarkably successful mapping the floodplain wetlands of the central Amazon basin using only two L-HH radar mosaics.

Therefore, to achieve the objective of a rapid, regional-scale method of tropical wetland classification, two L-HH radar datasets from the JERS-1/SAR GRFM Africa project were selected as the primary source of wetland information. Given the consistent confusion of non-floodplain forest with floodplain forest classes in previous radar floodplain wetland studies of the central Congo and Amazon basins (De Grandi et al. 2000a, Mayaux et al. 2002, Hess et al. 2003), and given the improvement that topographic information provides (Ozesmi and Bauer 2002, Hamilton et al. 2007), the addition of elevation data (HydroSHEDS DEM) and elevation derivatives (slope, HydroSHEDS Rivers, SRTM Water Bodies, for details see section 2.3.1) have also been selected as sources of wetland information. The rapid and transparent integration and analysis of these datasets is possible with an object-oriented approach (e.g., Hess et al. 2003, Hamilton et al. 2007, Durieux et al. 2007).

To address the first research question, appropriate classes for hydrologists, biogeochemists, and conservationists will be achieved by mapping similar classes to Hess et al. (2003). To adapt the classifier of Hess et al. (2003) to the varied hydrological conditions captured in the radar imagery of the Congo, the flooded and nonflooded hydrologic states of the vegetation classes must be eliminated, simplifying the classifier to 7 classes from 13. This simplification removes the requirement of an area to transition from nonflooded to flooded from the low-water to high-water mosaics, and instead indicates that an area was flooded in one or the other or both (see Data Analysis and Figure 2.8 below for more detail). The addition of topographic datasets also helps to distinguish classes and improve accuracy.

To address the third research question of reaching the best compromise between rapid analysis, thematic detail and accuracy, three maps of decreasing thematic detail of 7, 5 and 3 wetland classes are compared to similarly reclassified reference maps in order to determine the effect of a reduced number of classes on different measures of accuracy.

The study area, datasets, dataset preparation, analysis, and accuracy assessment are described in further detail below.

2.2 Study Area

The Equateur Province is an administrative area of the D. R. Congo located in the centre of the 500 m elevation contour of the Congo River basin (Figure 2.1). It is approximately 100,000 km^2 in size and is representative of many wetland types. As a part of the central basin, Equateur has been included in previous wetland descriptions and remote sensing products (Hughes et al. 1992, De Grandi et al. 2000a, Mayaux et al. 2000, Mayaux et al. 2002). These qualities make it an excellent test area for a method of wetland delineation, classification, and validation in this otherwise little studied basin.

2.2.1 Physical Setting

As its name implies, Equateur straddles the equator and extends from approximately 2°N to 2°S and from 16°E to 21°E. Equateur experiences 1800-2400 mm of rainfall per year (Runge 2007) with mean annual temperatures of 25 to 27°C that change little seasonally (Bultot 1971).

The portion of the Congo River that passes through this region is known as the Middle Congo, and is characterized by very low slope (1/15,000) and slow flow, with practically lacustrine conditions surrounding the islands of this approximately 15 km-wide, anastomosing reach (Hughes et al. 1992, Figure 2.2). The Congo River flows from Sumba Island in the northeast to a small town called Yumbi in the southwest of Equateur (Figure 2.2). At Mbandaka, the Congo River

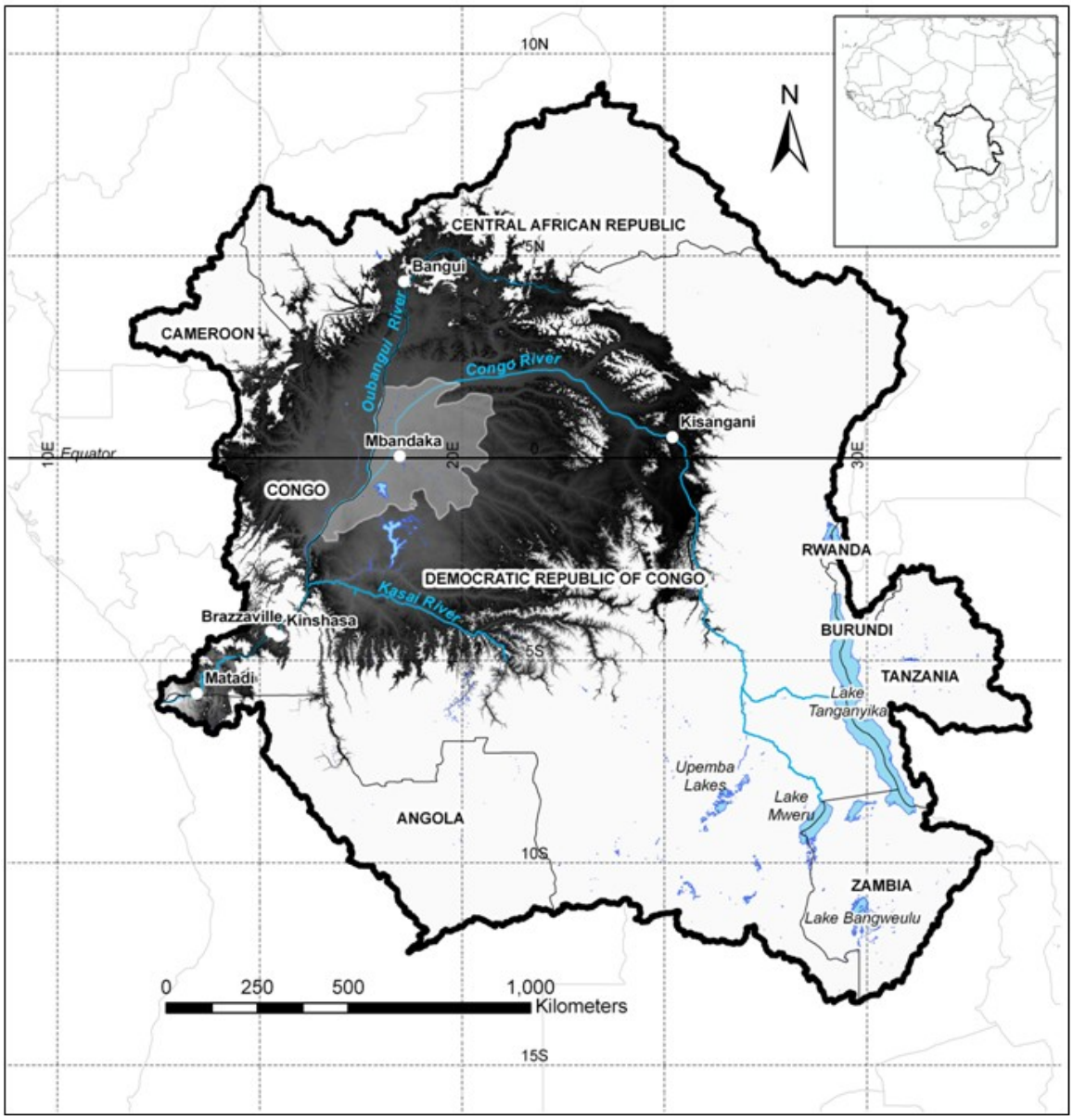

Figure 2.1: Selected political and physical features of the Congo River basin. The Equateur Province is highlighted in light grey within the 500 m elevation contour (grey-black area) of the basin.

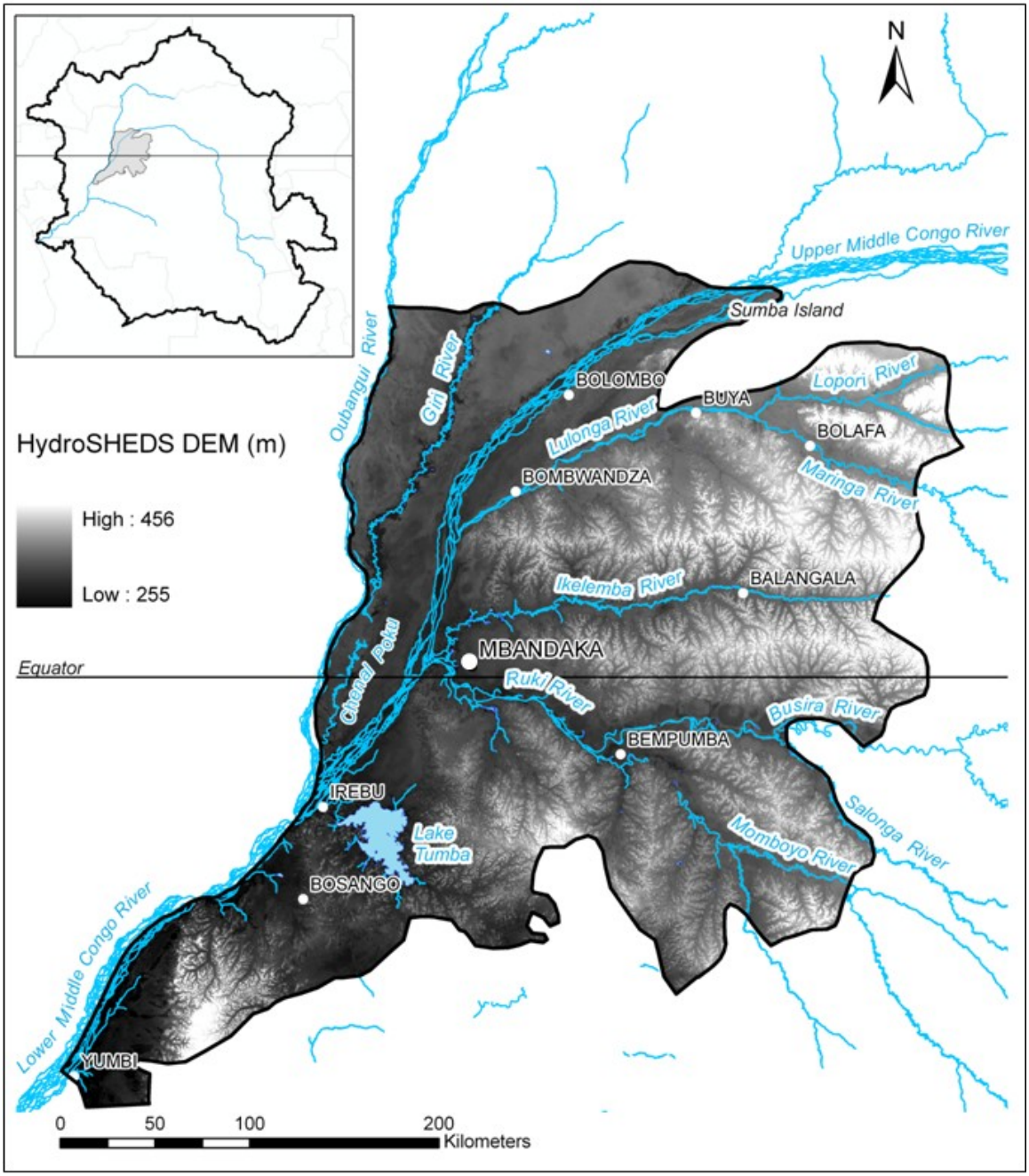

Figure 2.2: Rivers, lakes and settlements of Equateur Province, D. R. Congo. The Congo River flows from the northeast to the southwest.

has an average annual stage rise of 1.8 m, which is much less than the 15 m found at Manaus on the Rio Negro of the Amazon (Campbell 2005).

The confluence of the largest tributary of the Congo River, the Oubangui, as well as the Giri, Lulonga, Ikelemba, and Ruki Rivers occur in Equateur (Figure 2.2). Since the Congo River crosses the equator twice with large tributaries flanking on either side, Equateur tributaries show both uni-modal and bi-modal discharge patterns depending on their size and location relative to the equator. The right-bank tributaries (the Oubangui and Giri Rivers) both show unimodal hydrographs (Runge 2007). The Oubangui has the largest floodwave in the basin, rising up to 8 m in October and November with a stage low in March and April (Runge and Nguimalet 2005). The left-bank tributaries (Lulonga, Ikelemba and Ruki Rivers) of this region share bimodal discharge patterns, with peaks occurring from November to January and a lesser peak in March to May (Rosenqvist and Birkett 2002). Lake Tumba, the second largest lake of the central basin at approximately 500 km^2, lies in the southern portion of Equateur.

The alluvial plains of the middle Congo, Oubangui and Giri are composed of sands and clays high in organic matter (Campbell 2005). Sands dominate in the alluvium of the southern tributaries, and in some backwater swamps peat deposits occur up to 17 m deep (Campbell 2005). The waters of the central Congo River are black with relatively high dissolved organic matter (5 mg/L)

comprising 86% of its total organic carbon load, comparable to the Rio Negro of the Amazon (Coynel et al. 2005).

2.2.2 Central Congo Floodplain Wetlands

The Middle Congo exhibits extensive wetlands. On the right bank, where the Oubangui River converges with the Congo, 231,000 ha of flooded forest and perhaps another 100,000 ha in minor riparian swamps are estimated to occur (Hughes et al. 1992). The wetlands associated with this river are similar to those associated with the Congo mainstem, i.e., fringing flooded forest. Behind the levees of the Oubangui are backwater swamps that are periodically flooded and can extend up to 35 km from the river (Hughes et al. 1992).

The Giri River drains the area between the Oubangui and the Congo Rivers, joining with the Oubangui shortly before its confluence with the Congo River. The Giri is unique in this region for its extensive shrubs and herbaceous vegetation in its floodplain, in addition to having several channels connecting it with the Congo River as it meanders between the Oubangui and the Congo (Hughes et al. 1992). There are approximately 3 million ha of waterlogged flooded forest area between the Congo, Giri and Oubangui Rivers, forming a triangle of flooded forest from the confluence of the Congo and Oubangui approximately 375 km long and 165 km across (Hughes et al. 1992).

Of the left bank tributaries, the Ruki and Lulonga Rivers both exhibit extensive flooded forest at their confluences with the Congo River, along their lengths and beyond along the convergence of their tributaries: the Momboyo and Busira of the Ruki River, and the Maringa and Lopori of the Lulonga River. The largest continuous area of permanently and seasonally flooded forest occurs along the left bank of the Congo River immediately south of the Ruki, covering about 5 million ha and surrounding Lake Tumba (Hughes et al. 1992).

2.3 Methods

All datasets were prepared using the Mercator projection and the WGS84 datum in the geographic information systems suite ESRI ARC/INFO v. 9.3 © as described in "Data collection and preparation" below. All datasets except the reference dataset were analyzed in the Definiens Professional v. 5.0 © object-oriented software package as described and presented in Figure 2.3 below and in the following section, "Data analysis." Finally, the resulting wetlands map, herein referred to as the Equateur map, was exported back to ESRI ARC/INFO v. 9.3 © for reformatting in preparation for accuracy assessments that were executed in the IDRISI Andes 32 © software package using the error matrix (ERRMAT) module.

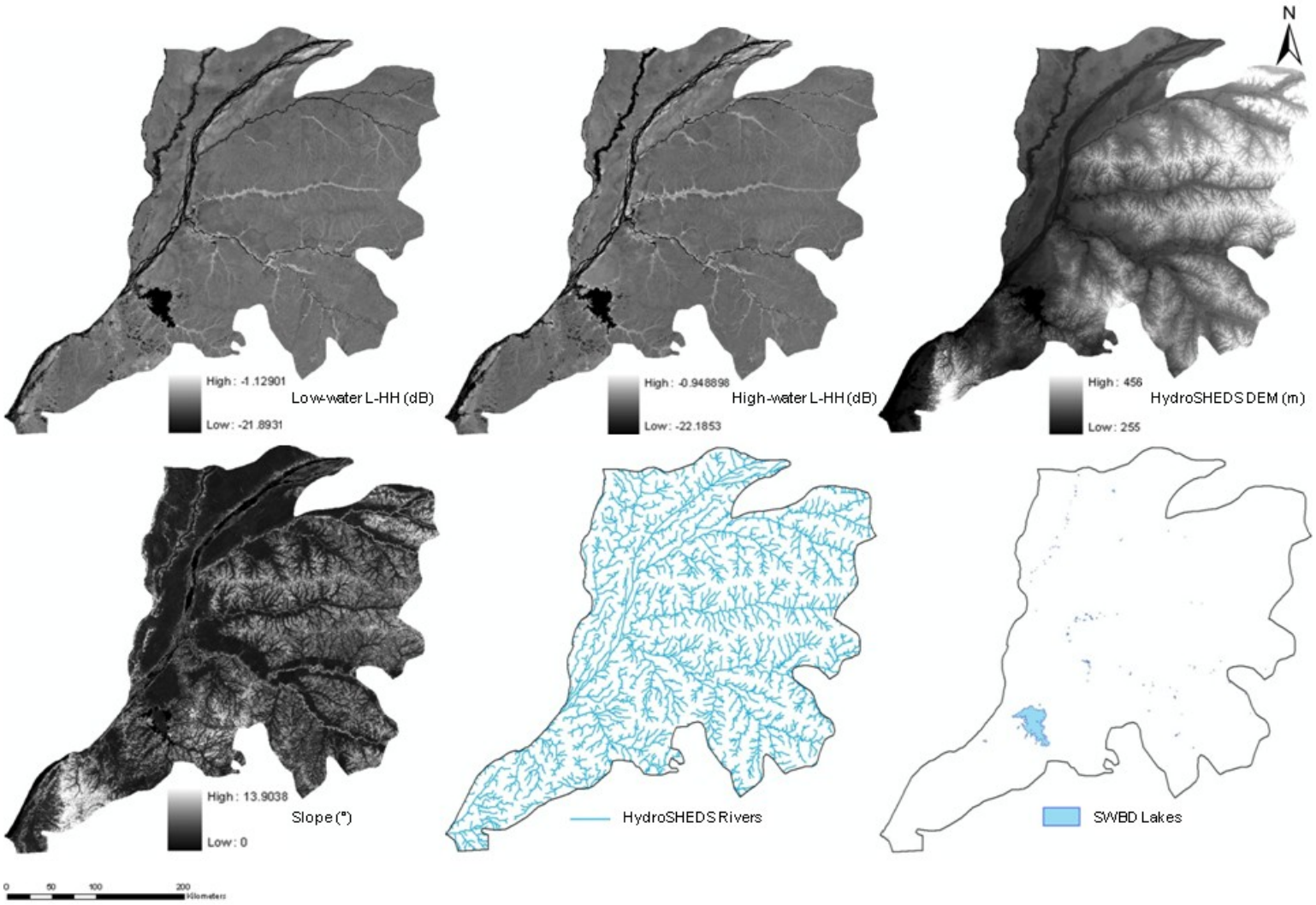

Figure 2.3: A visual overview of each dataset used for the Equateur floodplain wetland delineation and classification.

2.3.1 Data Collection and Preparation

2.3.1.1 JERS-1/SAR GRFM Africa Mosaics

Description

The main dataset used in this study for wetland information is from the Japanese Earth Resources Satellite Synthetic Aperture Radar sensor (JERS-1/SAR). One of its missions was to establish, for the first time, wall-to-wall estimates of the world's tropical forest using L-HH radar at high resolution (12.5 m). Known as the Global Rain Forest Mapping Project (GRFM), the mission imaged most of the tropics over its lifespan from 1992 to 1998. Several research centres were charged with developing custom algorithms to produce mosaics of acceptable radiometric and geometric calibration for particular regions. The European Commission Joint Research Centre (EC JRC) in Ispra, Italy, was responsible for the GRFM Africa products, which include two 8-bit mosaics downsampled to 100 m resolution over most of central Africa.

The two mosaics were compiled from over 3,900 scenes collected between January and March 1996 and again between October and November 1996. The collection of these scenes was from north to south, east to west, and it took approximately one month to image the whole basin once (Rosenqvist and Birkett 2002). While these mosaics are not "snapshots" of the hydrological and vegetation conditions across the basin, the timing of these collections was

designed to coincide with the low- and high-water conditions over the Congo River basin (Figure 2.3). Using correlations between altimeter readings (TOPEX/POSEIDON) and historical stage data, Rosenqvist and Birkett (2002) found that the mosaics represent high-water conditions in the basin well, but the "low-water" (January to March 1996) mosaic is not representative of actual low-water conditions in most areas. In Equateur, the Oubangui, Giri and Lulonga Rivers as well as the lower portion of the Congo River by Yumbi display good stage separation, whereas the stage separation upstream on the Congo River and the Ruki River is poor, and river stage separation is very poor (essentially unchanged between the mosaics) for the Busira and Maringa tributaries (Rosenqvist and Birkett 2002). Information does not exist on the stage separation for the Ikelemba River. This prevents the use of these mosaics to determine the full dynamics of flooding extent across Equateur (Hess et al. 2003). Ultimately, the complex hydrology of the basin makes bi-temporal mapping insufficient for flood extent studies in the Congo (Rosenqvist and Birkett 2002). Despite these shortcomings, the JERS-1/SAR GRFM Africa mosaics provide the most extensive and consistent source of radar data over the region, and the successor to the JERS-1/SAR, the ALOS/PALSAR, is designed to address this deficiency with new data products that can be incorporated into future analyses (see Discussion in Chapter 4).

Another important property of these data is that the mosaics are not orthorectified. This can cause geographic displacements in areas of high elevation, especially over mountainous terrain where the off-nadir angle of radar signals reflect off of steep slopes causing foreshortening and shadow effects. With the exception of mountainous areas, Birkett and Rosenqvist (2002) concluded that the geometric accuracy of the mosaics is still appropriate for hydrological applications and for use with other datasets. The absolute geolocation accuracy of the basin is 240 m, which is considered excellent for such a large area (De Grandi et al. 2000b). The 8-bit, 100 m data are available free for non-commercial purposes as a set of 15 tiles for each low and high-water season by request from the EC JRC.

Preparation

The metadata of the JERS-1/SAR GRFM Africa mosaics included the projection and coordinate information for each tile so that the entire mosaic could be reconstructed; however, the provided coordinates were not precise enough to do so. As suggested in the metadata, a manual “sliding” technique was needed to ensure that there were no gaps between the tiles. The coordinates of each tile were shifted to match seamlessly, without overlap, to the edges of the centre tile for both mosaics. The centre tile was chosen as the reference tile because it is most central to the basin and also happens to be where the majority of wetlands

occur. The cumulative error involved with sliding a set of tiles to a single reference tile is also reduced this way, and maximizes the cumulative error at the periphery of the basin where wetlands are least likely to occur. Ultimately the largest shift required was 70 m, or less than a pixel's distance.

The tiles were then merged to form a single mosaic for the low-water and also for the high-water conditions. Each mosaic was converted to normalized radar cross section (RCS) values, that is, from 8-bit digital numbers (DNs) to 32-bit floating point decibel (dB) values following an equation given in the metadata. The result is an improvement in scaling upon the 8-bit DNs, making them suitable for map-making using automatic supervised image classification such as in an object-oriented approach (De Grandi et al. 2000b).

The mosaics were then georectified to the SRTM Water Bodies dataset using thirty-six ground control points (GCPs) with at least one point from each tile (the characteristics of the SRTM Water Bodies dataset is given below). Areas of high elevation and mountainous terrain were avoided in this step since the mosaic tiles were not orthorectified and thus GCPs in these areas would affect the resulting error and transformation significantly. The mosaics were rectified using a cubic-convolution kernel and a third-order polynomial function. The residual mean square error was 87 m.

To improve computational efficiency and the stability of the image analysis program, the RCS-transformed data were subsequently converted to fit within an 8-bit range, while retaining the RCS values to one decimal place. The typical range for L-band radar data is approximately from -20 dB for areas such as water, to -3 dB for areas such as settlements and flooded forest. Therefore, a value of 25 was added to the RCS values to convert to positive values, and then the numbers were multiplied by 10 to preserve one decimal place, and finally the numbers were truncated to whole numbers to produce unsigned 8-bit data. (e.g., using [RCS + 25] * 10 with truncation, the RCS range of the low-water mosaic was transformed from {(-21.9) – (-1.2)} to {31 – 238}). Finally, the mosaics were clipped to Equateur's coverage.

2.3.1.2 HydroSHEDS DEM and Derivatives

Description

The HydroSHEDS project (Hydrological data and maps based on shuttle Elevation Derivatives at multiple Scales) (Lehner et al. 2006) provides several types of hydrographic information for regional and global-scale studies based on the Shuttle Radar Topography Mission (SRTM) Digital Elevation Model (DEM). The SRTM was flown by the space shuttle Endeavor for eleven days in February 2000. A Shortwave Infrared (SIR) C-band (5.3 cm) sensor imaged the elevation of the Earth between 60°N and S at 1-arc second (approximately 30 m)

resolution. It was a joint project between NASA (National Aeronautics and Space Administration), NGA (National Geospatial-Intelligence Agency of the U.S. department of defense), the German Aerospace Centre (DLR) and the Italian Space Agency (ASI). The SRTM 3-arc second (approximately 90 m) DEM was originally created by NASA's Jet Propulsion Lab (JPL) and processed to Digital Terrain Elevation Data (DTED) standards by NGA. More detail about the mission is provided in Farr and Kobrick (2000). The HydroSHEDS datasets of interest derived from the SRTM DEM are the HydroSHEDS DEM and HydroSHEDS Rivers, which were downloaded free of charge from the USGS SRTM HydroSHEDS server (http://hydrosheds.cr.usgs.gov/).

The HydroSHEDS DEM combines the advantages of the SRTM-3 and DTED-1 data because the SRTM-3 data are averaged and reduce radar noise while the DTED-1 was sampled and more clearly represents shorelines and waterbodies (Lehner et al. 2006). However, an important artifact of the source data is its inability to penetrate dense vegetation since the C-band wavelength cannot penetrate dense canopies such as tropical forest. This causes error in the height estimation, especially over areas such as the Congo floodplain forest where canopies can reach or exceed 40 m in height. For technical reasons the data were shifted 1.5 arc-seconds (approximately 45 m) to the north and east and each tile's overlapping right column and row were removed (Lehner et al.

2006). The HydroSHEDS Rivers dataset is based on a flow accumulation layer derived from the DEM data at 15 arc-second (approximately 450 m) resolution with a threshold of 100 upstream cells (Lehner et al. 2006) (Figure 2.3).

Preparation

Twenty-three tiles were required to cover the basin and were merged into a single mosaic. The mosaic was then reprojected using cubic-convolution resampling, shifted 45 m south and west to correct for the displacement in its production, and, along with the basin's HydroSHEDS Rivers dataset, clipped using the Equateur theme (Figure 2.3).

With the HydroSHEDS DEM of Equateur, a slope layer (in degrees) was produced. The 32-bit floating point dataset was transformed to 8-bit data by multiplying the result by 10 to preserve a decimal place and by truncating the number to provide a whole number, changing the range of slope from {0 – 13.9038} to {0 – 139} (Figure 2.3).

Since these datasets are based on the same elevation data as the SRTM Water Bodies (Lakes) dataset—the georeference dataset—georectification was not required or performed for the DEM or river network.

2.3.1.3 SRTM Water Bodies (Lakes)

Description

The SRTM Water Bodies Dataset (SWBD) was developed as a by-product of NGA's editing of the SRTM DEM. Ocean, lake and river shorelines were identified and delineated from 1 arc-second (approximately 30 m) DTED-2 data and saved as polygons. An important artifact of these data is the timing of the acquisition: the world's waterbodies are delineated as they appeared in February 2000. The accuracy of the dataset is within 20 m in the horizontal and 16 m in the vertical direction (SWBD 2003). Only lakes greater than 600 m in length and 183 m in width are included. Islands with a medial length greater than 300 m are included, as are smaller islands if more than 10% of the area exceeds 15 m above the surrounding water. The dataset used in this study had all river polygons, which are also part of SWBD, removed previously.

Preparation

The SWBD Lakes dataset was clipped to the Equateur region.

2.3.1.4 Reference Map dataset: FAO Africover

Description

The United Nations Food and Agriculture Organization (FAO) began a landcover mapping initiative for Africa to improve the natural resource management of this data-poor region. The FAO Africover project began with

countries in east and central Africa with the eventual goal of creating an Africa-wide, exhaustive, multi-purpose landcover map (Di Gregorio and Jansen 2005). The maps are derived separately for each country using optical, 30 m (LANDSAT) imagery as the data source. The imagery is interpreted and digitized into polygons by local experts according to the UN's Land Cover Classification System (LCCS) with the flexibility of custom classes where deemed appropriate.

The LCCS proceeds in two phases. The first phase is strictly dichotomous which sorts a polygon in three steps, producing eight basic classes (Figure 2.4). The second phase of classification is also hierarchical but the classifiers are specific to each of the eight basic classes (Figure 2.4). Many classifications are possible; for the Africover data available for the D. R. Congo, for example, over 80 classes are used, approximately twenty of which could be considered wetland (i.e., a vegetated area that is flooded for at least 2 months of the year). The accuracy of the dataset is reported to exceed 60% for the eight primary classes derived from the first phase of classification, but no accuracy assessment has been conducted for the classes derived in the second phase of classification (Di Gregorio and Jansen 2005).

Each polygon has at least one classification. It is possible to have more than one classification in the case that a feature is too small to be mapped alone according to the minimum mapping area used. The minimum mapping area

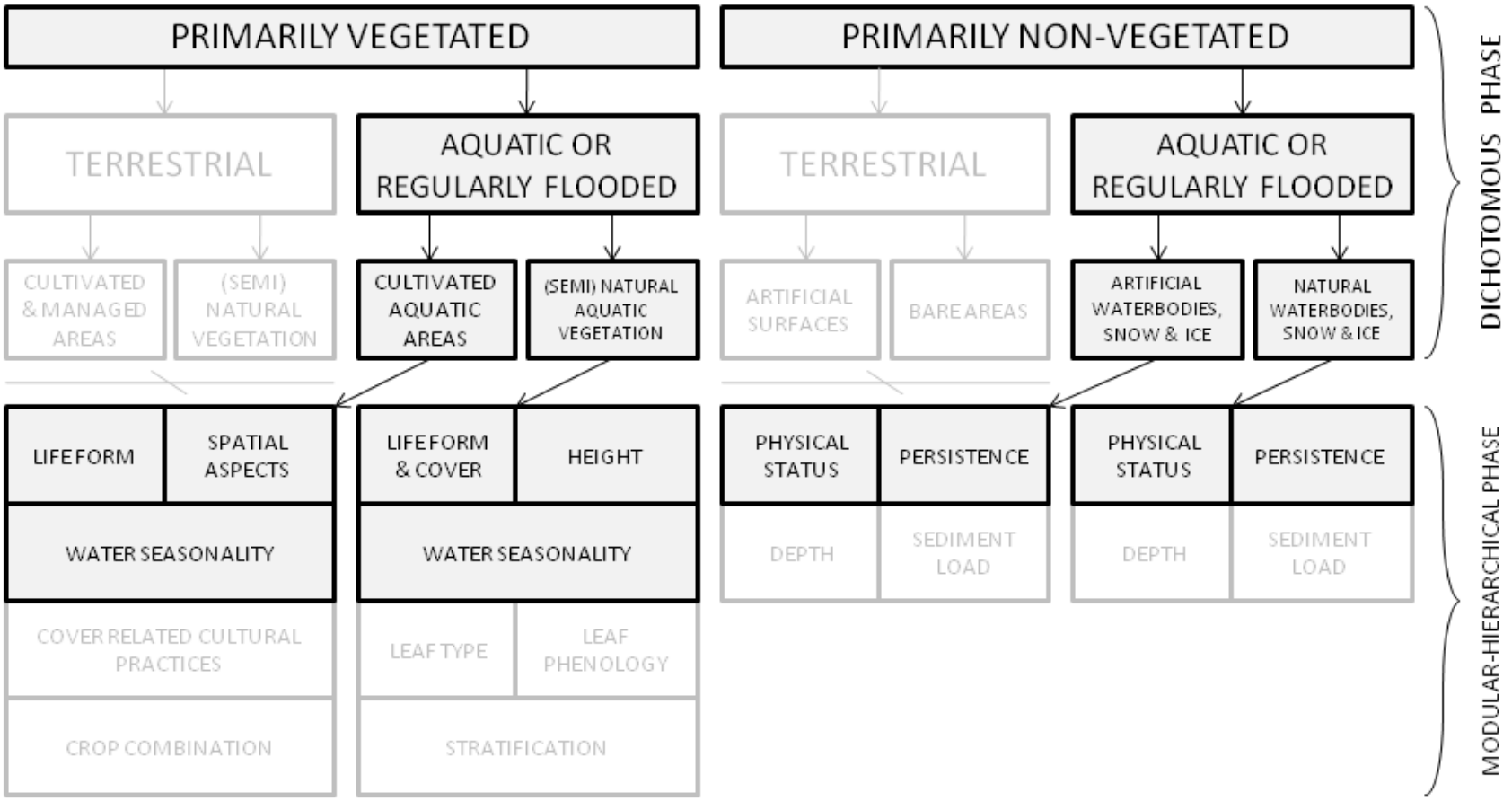

Figure 2.4: Landcover classification key according to the UN LCCS as used for reclassifying wetland polygons in the D. R. Congo Africover dataset. The classifiers used for wetland reclassification are highlighted in the black boxes, whereas the terrestrial branches of the dichotomous phase classification and the modular-hierarchical classifiers not used for wetland reclassification are faded in grey boxes.

(MMA) concept is applied by cartographers when addressing the smallest area that can be shown on a map (Di Gregorio and Jansen 2005). In Equateur, the MMA of wetland classes is 34 ha. In the case of two classifications given for a polygon, one feature dominates the cover of the other within the polygon, and the second cover still covers at least 20% of the polygon (Di Gregorio and Jansen 2005). In the case of three classifications, the dominant feature approximates 40% cover, while the remaining two features each approximate 30% cover (Di Gregorio and Jansen 2005). However, no polygons were composed of three features in the Equateur Province. This mixed mapping unit description allows some degree of fuzziness or thematic uncertainty to be expressed in the polygon classification (Di Gregorio and Jansen 2005).

The imagery used for creating the D. R. Congo Africover portion of the Equateur Province was collected from 2000 to 2001 (Figure 2.5). With no seasonal or annual consistency between the scenes, interpreting the hydrology classifier of potential wetland polygons bears a few caveats. Firstly, as the scenes are not from a single season, the hydrological conditions across Equateur are not consistent. Secondly, the hydrology classifier has three levels: inundation for at least 2 months of the year; inundation between 2 and 4 months of the year; and waterlogged conditions. Since the imagery is not multi-temporal, there is no way to ascertain the length of time an area has been flooded for. This is in

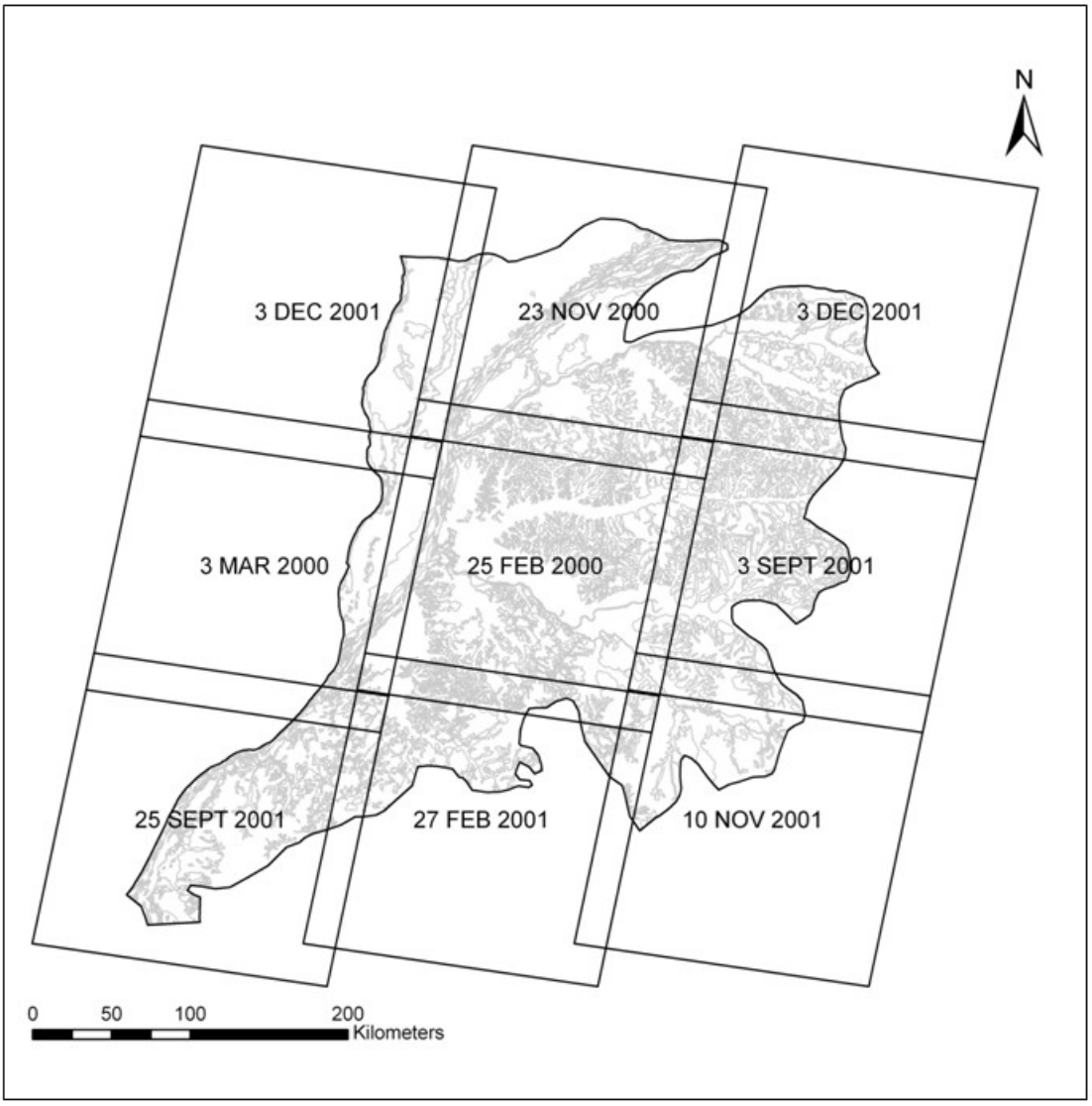

Figure 2.5: LANDSAT scene acquisition dates used for the visual interpretation of landcover classes for Africover (in grey polygons) in Equateur.

addition to the difficulty of determining the extent of flooding under vegetation canopies using optical imagery. Therefore, it is assumed that the hydrology classifier was based upon the expert knowledge and interpretation of wetland vegetation as an expression of flooding characteristics.

Preparation

The full-resolution datasets for the D. R. Congo were received free of charge from the Africover program. All records were clipped using the Equateur theme. Additional fields were added to reclassify polygons according to the hydrology-physiognomy class definitions adapted from Hess et al. (2003) (see following section), following the rules shown in Figure 2.6 in the event of mixed mapping units.

It is also important to note that no ground-truthing was conducted in this area to verify the accuracy of this classification. Africover has been sparsely ground-truthed in general. An obvious example is the upland classification of the areas between the Congo, Giri and Oubangui Rivers. According to the original Africover data, the polygons in this area do not have any element of flooding. However, this area is well documented as one of the largest continuous expanses of permanently and seasonally flooded forest in the central basin (Hughes et al. 1992), and has been classified as such in independent satellite

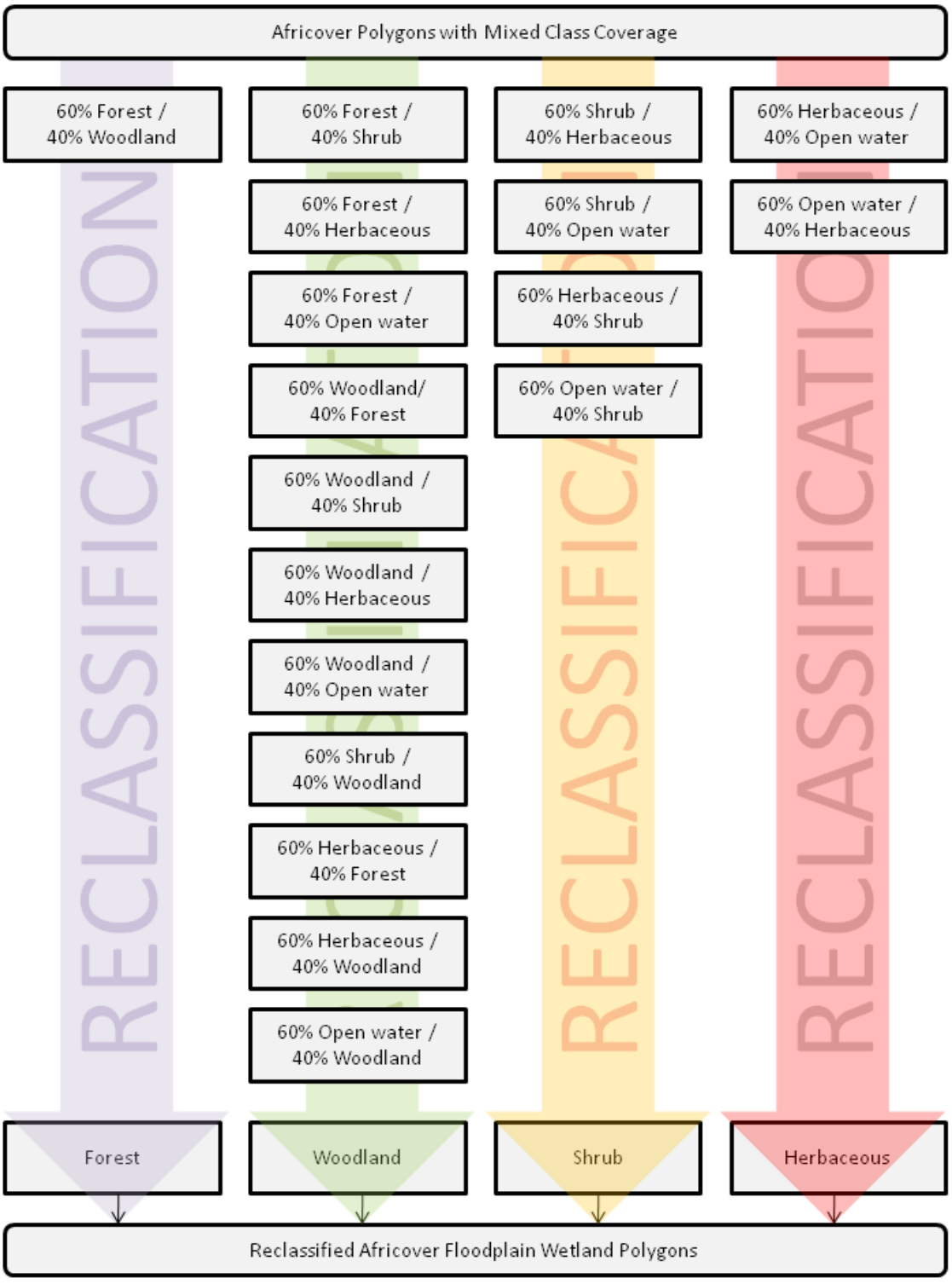

Figure 2.6: Reclassification rules of Africover mixed mapping units.

studies of flooded forest in the region (De Grandi et al. 2000a, Mayaux et al. 2000, Mayaux et al. 2002, Vancutsem et al. 2009). Therefore the largest polygons of this area were considered misclassified and were reclassified from upland to floodplain forest for comparison to the Equateur map (Figure 2.7).

2.3.2 Data Analysis

2.3.2.1 Adapted Classifier from Hess et al. (2003)

The physiognomic-hydrologic scheme employed by Hess et al. (2003) follows the "functional parameterization" (Sahagian and Melack 1998) of wetlands suitable for hydrological and carbon biogeochemical modeling (Melack and Forsberg 2001), fish habitat quality, and the occurrence of agricultural potential (Gutjahr 2000). The classifier was derived from the dual-season GRFM Amazon L-HH RCS probability density functions (PDFs) of 13 different environments in the central Amazon basin (Tables 2.1 and 2.2). The parallel-piped classifier makes the decision boundaries between classes transparent and easily modified (Hess et al. 2003, Figure 2.8). However, the hydrologic component of this classifier assumes a consistent, unidirectional rise in river stage from one radar mosaic to another, which does not hold true for the GRFM Africa L-HH mosaics over most of the Congo basin and Equateur region (Rosenqvist and Birkett 2002).

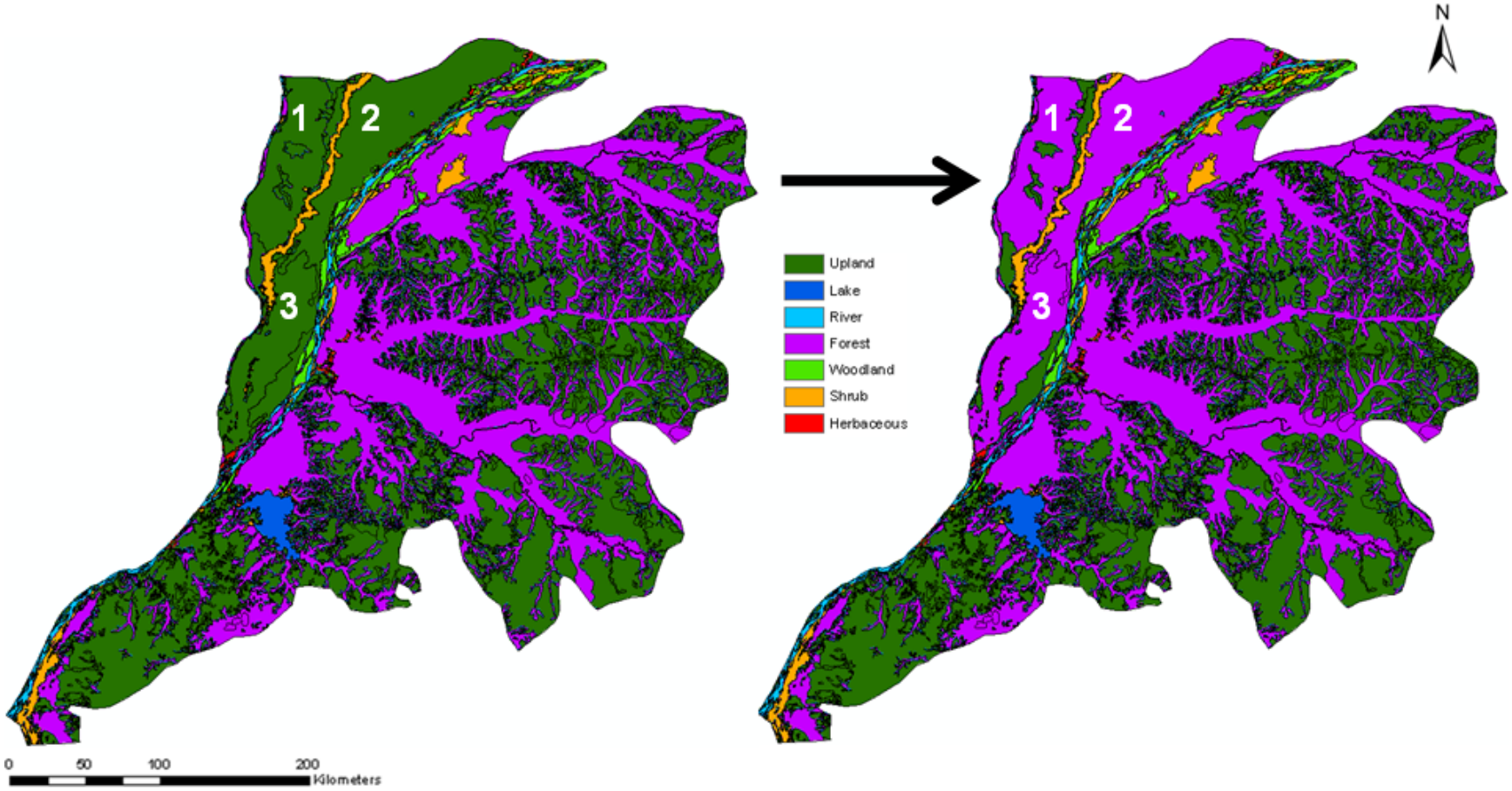

Figure 2.7: The three polygons reclassified from upland to floodplain forest. Data source: FAO Africover.

Table 2.1: Definitions of hydrology, life forms and classes of Equateur wetlands map (adapted from Hess et al. 2003) and the UN LCCS (as used in Africover).

	TERM	EQUATEUR DEFINITION	AFRICOVER DEFINITION
HYDROLOGY	Flooded	Water table is above surface; instantaneous in either radar mosaic	Water table is at or near surface for > 2 mo./yr.; implied through vegetation
LIFE FORM	Tree	> 5 m, woody, single stem	> 5 m, woody
	Shrub	0.5 to 5 m, woody, bushy	0.3 to 5 m, woody
	Herbaceous	Non-woody	0.03 to 0.3 m, non-woody
CLASS	Upland	Not flooded on either date; not consistent with floodplain geomorphology	Polygon does not experience any flooding.
	Open water (lake, river)	< 1% vegetation cover	< 4% vegetation cover > 10 mo./yr
	Floodplain forest	Closed tree canopy (60 - 100%)	Closed tree canopy (60/70 - 100%);
	Floodplain woodland	Open tree canopy (25 - 60%)	Open tree canopy (10/20 - 60/70%);
	Floodplain shrub	Closed to open shrub canopy	Closed to open shrub canopy
	Floodplain herbaceous	< 25% woody canopy cover, >25% herb. Cover	Closed to open herbaceous canopy

Table 2.2: LCCS labels used for reclassification of the Africover dataset.

Reclassified as	Map Code	LCCS Label
Lake	7WP	Artificial Perennial Waterbodies (Standing)
	8WP	Perennial Natural Waterbodies (Standing) Salinity: Fresh, < 1000 ppm of TDS
	8WN	Non-Perennial Natural Waterbodies (Standing)
River	8WFP	Perennial Natural Waterbodies (Flowing) Salinity: Fresh, < 1000 ppm of TDS
	8WFN2	Non-Perennial Natural Waterbodies (Flowing) (Surface Aspect: Bare Soil)
	8WFN1	Non-Perennial Natural Waterbodies (Flowing) (Surface Aspect: Sand)
Forest	4TCFF1Y	Broadleaved Evergreen Forest On Permanently Flooded Land/Water Quality: Brackish
	4TCIFF1-rh	Broadleaved Evergreen High Forest On Permanently Flooded Land (Persistent)/Water Quality: Fresh/Floristic Aspect: Raphia L.
	4TCIF1	Broadleaved Evergreen High Forest On Temporarily Flooded Land/Water Quality: Fresh
	4TCMF218	Semi-Deciduous Medium High Forest With High Shrubs On Temporarily Flooded Land/Water Quality: Fresh
	4TCIFF18	Broadleaved Evergreen High Forest With High Shrubs On Permanently Flooded Land/Water Quality: Fresh
Woodland	4TPMFF18	Broadleaved Evergreen Medium High Woodland With High Shrubs On Permanently Flooded Land/Water Quality: Fresh
	4TPMF218	Semi-Deciduous Medium High Woodland With High Shrubs On Temporarily Flooded Land/Water Quality: Fresh
Shrub	4SCJFF	Closed Medium To High Shrubs On Permanently Flooded Land/Water Quality: Fresh
	4SCJF	Closed Medium To High Shrubs On Temporarily Flooded Land/Water Quality: Fresh
	4SPJFF6	Open Medium To High Shrubs With Medium To Tall Herbaceous Vegetation On Permanently Flooded Land/Water Quality: Fresh
	4SPJF6	Open Medium To High Shrubs With Medium To Tall Herbaceous Vegetation On Temporarily Flooded Land/Water Quality: Fresh
Herbaceous	4H(CP)FF	Closed to Open Herbaceous Vegetation On Permanently Flooded Land/Water Quality: Fresh Water
	4HCF	Closed Herbaceous Vegetation On Temporarily Flooded Land/Water Quality: Fresh
	4FCLFF-j	Closed Short Forbs On Permanently Flooded Land (Persistent)/Floristic Aspect: Jacintus sp.
	4HPJFF	Open Medium To Tall Herbaceous Vegetation On Permanently Flooded Land (Persistent)/Water Quality: Fresh
	4HPJF	Open Medium To Tall Herbaceous Vegetation On Temporarily Flooded Land/Water Quality: Fresh
	4H(CP)F8	Closed to Very Open Herbaceous Vegetation With Sparse Shrubs On Temporarily Flooded Land/Water Quality: Fresh Water

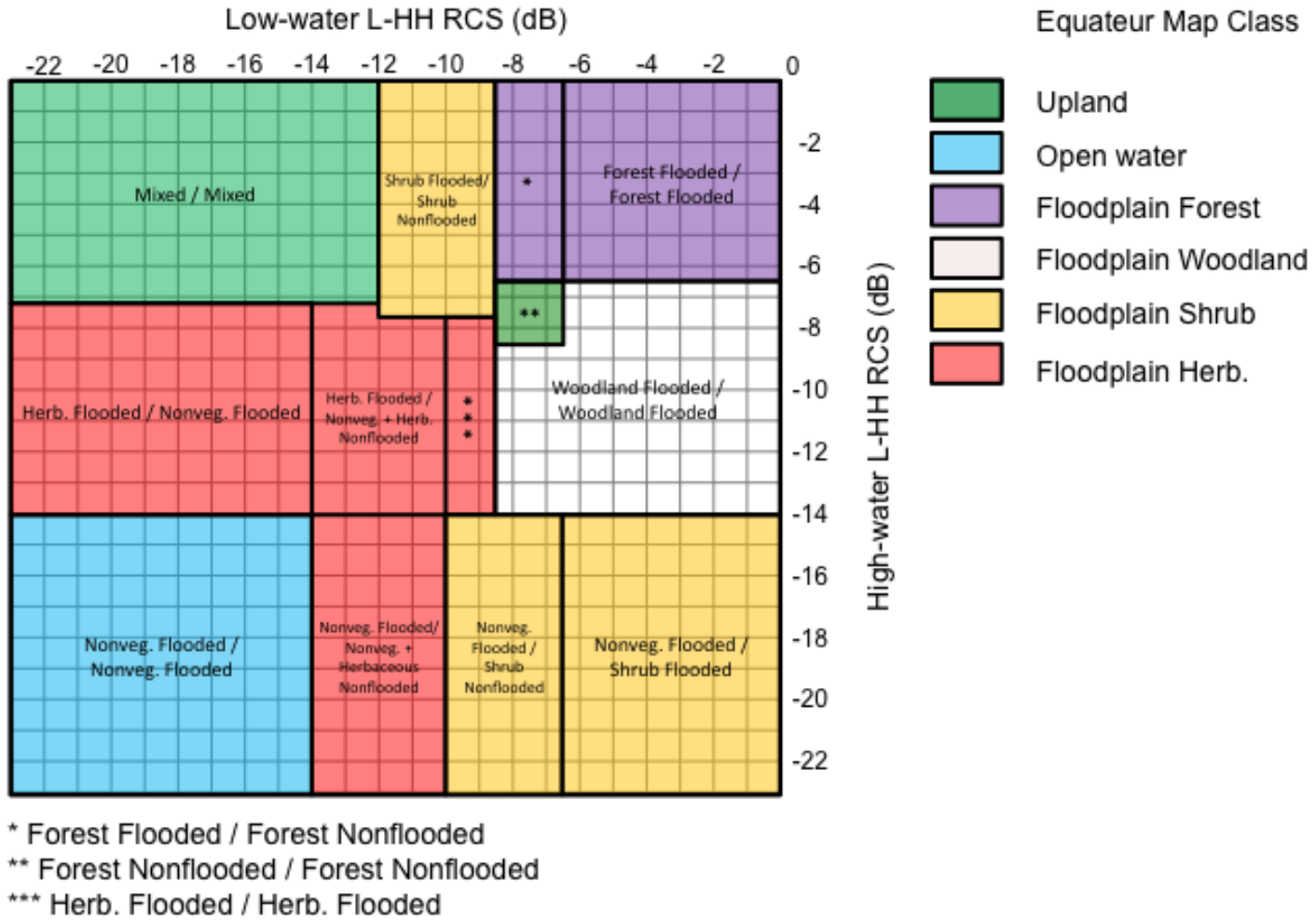

Figure 2.8: The parallel-piped classifier of Hess et al. (2003) with the original class labels superimposed over their colour-coded aggregation as used in the Equateur method.

In order to meaningfully adopt the classifier of Hess et al. (2003), the flooded and nonflooded hydrologic states of the vegetation classes are combined, simplifying the classifier into 7 classes from 13 (Figure 2.8). This simplification removes the requirement of a vegetated area to transition from nonflooded to flooded in the low-water to high-water mosaics, and instead indicates that an area is flooded in one or the other or both. When transferring this classifier from the floodplain environments of the central Amazon to the central Congo, the assumption is made that the vegetation structure and flooding response in the radar mosaics remains the same for each class, which may not hold true if canopy structure or densities differ between the same physiognomic classes (e.g., forest) as a result of different floristics (i.e., species), for example.

2.3.2.2 Segmentations and classifications

After preparation, all of the datasets except the reference dataset were loaded into the object-oriented software, which is capable of integrating raster and vector datasets of different spectral and spatial resolutions while taking into account other contextual information.

The fundamental step in an object-oriented approach is the segmentation of an image into homogenous regions, or objects. Unlike pixel-based classification, segmentation is a region-growing method that starts with a single pixel and aggregates neighbouring pixels into objects provided that their value

meets the level of homogeneity with their neighbour as specified by the analyst. It therefore asserts that images are made up of regions and separated by edges within which a parameter such as the RCS is constant (Oliver and Quegan 1998). Image segmentation is the most important step of an object-oriented approach because it produces the fundamental units for classification.

Five segmentation levels were used in this study (consult Figure 2.9 for details to the following explanations). The first segmentation reduced the number of objects to a computationally manageable number, as well as distinguished areas within Equateur from areas outside of Equateur. (The object-oriented software still considered data imported as “no data” as real data.)

The second segmentation derived upland objects (Figure 2.9). Finding the appropriate layers, scale and shape factors to segment an area into objects that reflect landscape units is a process based on inference and trial and error. This was the most experimental and crucial step of the segmentation processes because the objects derived at this level were the objects on which the landcover classifiers acted.

A third segmentation procedure was necessary to delineate open water objects since radar data, not elevation data, are most sensitive to this feature. Lake and river objects were further distinguished using the SWBD Lakes dataset (Figure 2.9).

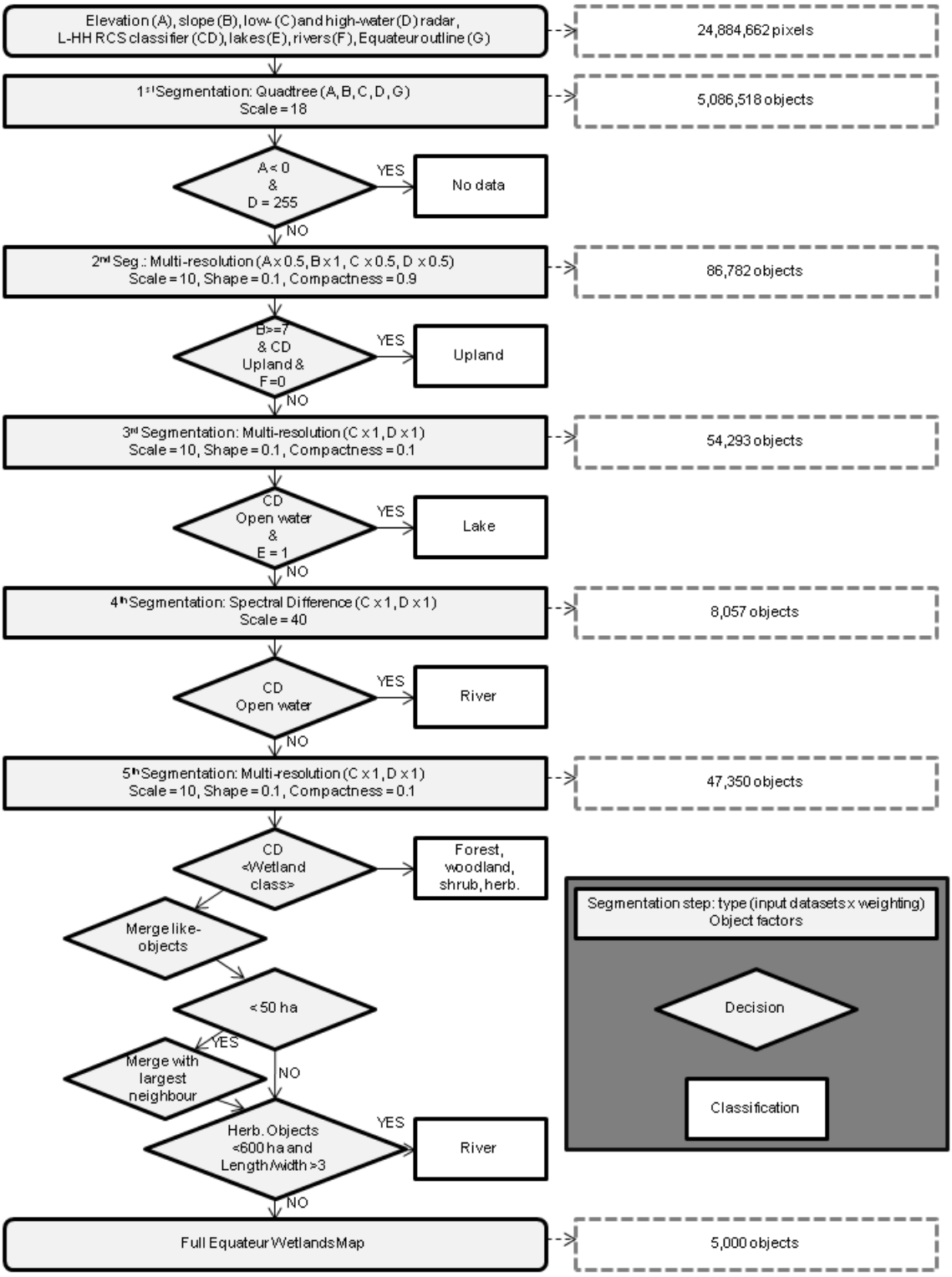

Figure 2.9: Flowchart of the segmentation and classification rules. A legend is highlighted in the dark grey box.

A fourth, growing-region segmentation was applied based on the spectral difference between unclassified objects (Figure 2.9). This effectively merged objects with neighbouring objects that are most spectrally similar based on a user-defined threshold. This extra grow-region segmentation produced a more continuous and robust river classification based on the open water RCS ranges in the parallel-piped classifier. Since the grow-region segmentation merged objects to a level too large for appropriate wetland classification, a fifth and final segmentation was required for floodplain wetland classification.

The fifth and final segmentation derived floodplain wetland objects. The fifth segmentation procedure was exactly the same as the third, using only information from the radar mosaics (Figure 2.9). Only radar information was required at this level because floodplain wetland objects were classified according to their mean RCS given by the classifier adapted from Hess et al. (2003). Since the thresholds are crisp and do not overlap (i.e., not fuzzy), the order of floodplain wetland object classification was not important, but for purposes of clarity, were classified in the order of: forest, woodland, shrub, and lastly, herbaceous vegetation.

After all segmentation and classification steps were completed, a minimum mapping area of 50 ha for all classes was enforced, following Mayaux et al. (2002) and Hess et al. (2003) (Figure 2.9).

Finally, as there remained considerable confusion between the river and herbaceous classes at this stage, an additional rule reclassified all smaller, thinner herbaceous objects as river objects (Figure 2.9).

2.3.2.3 Simplified Wetlands Map and Basic Floodplain Map

Two additional maps were produced from the full, seven-class Equateur map described above, namely a “simplified” wetlands and a “basic” floodplains map. Both contain fewer classes as the result of combining classes in strategic ways.

The simplified wetlands map contains five classes and is based on the *a priori* knowledge that dual-season L-HH mosaics are excellent for mapping flooded trees but have difficulty distinguishing between shrub and herbaceous vegetation (Hess et al. 2003). Therefore, this map combines the floodplain forest with the floodplain woodland classes to effectively create a floodplain trees class, termed “tall vegetation.” The floodplain shrub and herbaceous classes are also combined to form the “short vegetation” class. The simplified wetlands map maintains the upland, lake and river classes from the Equateur map without any change.

The basic floodplain map reduces the number of classes to three to test the ability of the Equateur method to distinguish the floodplain environment from upland and open water. It could effectively serve as a wetland mask, for

example. A wetlands mask—or, in the case of the tropics, areas that are not a part of the floodplain,—would include areas that are vegetated but are not flooded in either radar mosaic nor are consistent with floodplain geomorphology (upland), as well as areas that are flooded in both mosaics but are not vegetated (open water). These two conditions translate into the two basic non-wetland classes of upland and open water and bound the floodplain environment as a result. This basic classification serves as a benchmark for maximum correspondence between the Equateur method and the reclassified Africover map.

2.3.3 Accuracy Assessment

The full Equateur map was exported from the object-oriented software as a raster file in a Mercator projection with 92.5 m resolution into the GIS in preparation for accuracy assessment. The Africover data were rasterized to 92.5 m pixels. The Equateur map was shifted east approximately 16.5 m and south 22.1 m to correspond areas of data and no data perfectly with the Africover map, as required for error matrix generation by the accuracy assessment software. To achieve this, both maps were masked so that only pixel locations that show data in both maps are preserved, and those pixels that overlap with “No data” in either map were eliminated. The class reductions to produce the simplified wetlands map and basic floodplain map and corresponding reference maps were

performed in the GIS with a straightforward reclassification command. All maps were imported into the accuracy assessment software, where three error matrices were produced, including measures of overall, producer's and user's accuracy as well as the Kappa Index of Agreement (KIA) between maps. Quantification, or total area, of each class for each map was also tabulated. The results for and interpretations of each map and each class are presented below.

3. Results and Interpretation

3.1 Full Equateur Wetlands Map

The full Equateur wetlands map includes seven classes: upland, lake, river, floodplain forest, floodplain woodland, floodplain shrub and floodplain herbaceous vegetation. It is the most thematically detailed map of the three produced in this study and is the source of the simplified wetlands map and basic floodplain map described further below. The Equateur wetlands map and corresponding Africover map are shown in Figure 3.1. The floodplain woodland class, however, was discovered to be a misnomer, and is more appropriately labelled nonflooded forest in contrast with floodplain forest, which is itself more appropriately labelled flooded forest, for reasons given further below.

The overall accuracy of the full Equateur wetlands map is 47% compared to the Africover reference map, with a KIA of 28% (Table 3.1). The majority of the overall map error is confusion between flooded forest and nonflooded forest pixels. The majority of nonflooded forest commission error (user's accuracy) (75%) and omission error (producer's accuracy) (73%) involves confusion with Africover's flooded forest class. Compared to Africover, the flooded forest class is underestimated by approximately 4,100,000 pixels, whereas nonflooded forest is overestimated by 4,400,000 pixels: nearly the same amount (Table 3.2).

Table 3.1: Error matrix and accuracy measures of the full Equateur wetlands map, in hectares.

		Reference Data							Classified
		U	L	R	Forest	Woodland	S	H	Total
Classified Data	U	**3,432,894**	344	3,215	920,936	51,431	10,571	2,472	4,421,863
	L	957	**75,316**	0	683	0	174	236	77,365
	R	13,244	119	**221,049**	18,304	11,376	8,289	6,039	278,420
	FF	124,565	1,538	30,763	**1,009,377**	118,199	73,279	11,112	1,368,833
	NF	1,000,673	606	5,762	2,905,147	**29,798**	52,991	8,736	4,003,713
	S	2,839	46	91	1,755	263	**32,101**	857	37,952
	H	46,161	731	3,367	12,285	631	61,857	**7,433**	132,466
Reference Total		4,621,333	78,699	264,247	4,868,487	211,698	239,263	36,885	**10,320,612**

		Producer's Accuracy	User's Accuracy
U	= Upland	74%	78%
L	= Lake	96%	97%
R	= River	84%	79%
FF	= Fl. Forest	21%	74%
NF	= Nonfl. For.	14%	1%
S	= Shrub	13%	85%
H	= Herbaceous	20%	6%

Overall Accuracy	**47%**
KIA	**28%**

Table 3.2: Comparison of quantity between the mapped and reference full Equateur wetland classes.

Class	Mapped ha (M)	Reference ha (R)	Difference (D = M - R)	% Difference (%=D/R*100)
Upland	4,421,863	4,621,333	-199,470	**-4**
Lake	77,365	78,699	-1,334	**-2**
River	278,420	264,247	14,173	**5**
Flooded Forest	1,368,833	4,868,487	-3,499,654	**-72**
Nonfl. Forest	4,003,713	211,698	3,792,015	**1791**
Shrub	37,952	239,263	-201,311	**-84**
Herbaceous	132,466	36,885	95,581	**259**

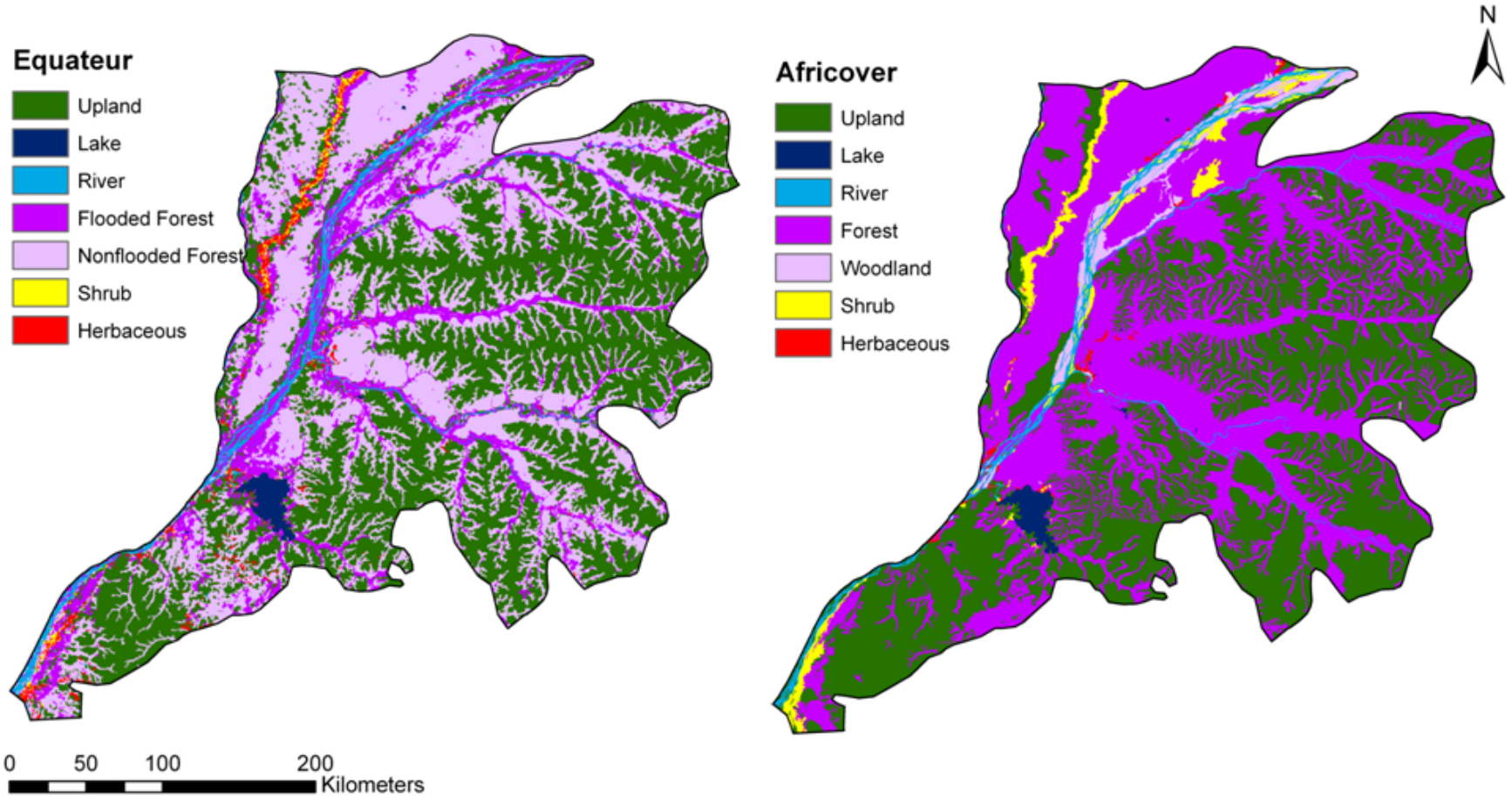

Figure 3.1: A visual comparison of the full Equateur wetland map and the reclassified Africover reference map.

3.1.1 Floodplain Forest and Woodland Misclassifications

Several sources indicate that almost the entire floodplain is covered by closed forest canopy and is either permanently or intermittently flooded (Hughes et al. 1992, De Grandi et al. 2000, Mayaux et al. 2002). This is in agreement with Africover (Figure 3.1). According to the parallel-piped classifier adapted from Hess et al. (2003), the majority of the floodplain environment is considered floodplain woodland, or to have a tree canopy cover between 25% and 60% and to be semi-permanently to permanently flooded. Because no ecological distinction is made in descriptive (Hughes et al. 1992) or visual (De Grandi et al. 2000, Mayaux et al. 2002) accounts of the area that explain the pattern of floodplain forest and woodland shown in the Equateur wetlands map, it is likely that ecologically there is little or no difference between the vegetation type or canopy closure of the forest and woodland classes.

While the vegetation classification is the same, the hydrological classification is not. The hydrological definitions and indicators differ: for an Equateur object to be classified as flooded, the area must show water above the surface at the time of observation; for an Africover polygon to be classified as flooded, its hydrology is inferred from vegetation that indicates the area has a water table at or near the surface of the ground not necessarily at the time of observation, but for at least two months of the year. Therefore, the hydrology

classifiers differ with respect to time: the Equateur classifier is based on two instantaneous points in time, whereas the Africover classifier is not one of flood extent but hydrophytic vegetation extent. This explanation is consistent with the distribution of floodplain forest in the Equateur wetlands map, where the brightest floodplain wetlands are next to rivers. This is expected when interpreting L-HH radar response. Since floodplain woodland is likely the same or similar to floodplain forest in vegetation structure and canopy closure, floodplain woodland is a misnomer: in the Equateur wetlands map, it is likely also floodplain forest, but nonflooded. Although the remaining misclassifications in other classes are comparatively minor in relation to this error, the accuracies and their likely explanations are provided below.

3.1.2 Upland

For the upland class, producer's and user's accuracies are approximately equal at 74% and 78% respectively (Table 3.1). In both cases, the majority of the error is the result of confusion with a single class. About 84% of the error associated with producer's accuracy (omission error) is confusion with nonflooded floodplain forest (formerly floodplain woodland). Approximately 93% of the error associated with user's accuracy (commission error) is confusion with Africover's forest class. In terms of quantification, the Equateur upland class

approximates Africover's upland class well with 4% fewer upland pixels (Table 3.2).

The source of greatest confusion is the difference between the distributions of upland and floodplain areas (flooded and nonflooded floodplain forest). While they generally approximate visually (Figure 3.1), there are explanations for their small though consistent discrepancies.

The first is that the boundaries of the largest upland areas are scaled back when compared to the Africover map (Figure 3.1). This is likely a result of the different sensitivities of L-HH radar and optical imagery to forest canopies, as well as a result of the subjective nature of delineating boundaries between landcovers with a relatively fuzzy transition in optical imagery, as the transition between forest types is extremely gradual in this region (Hughes et al. 1992). De Grandi et al. (2000a) found this to be the most likely explanation for the discrepancies between their C-VV radar-based swamp forest map and the optical imagery based reference map of the region. This explains much of why the quantity of upland is lower (by 4% or 233,350 pixels) and floodplain is higher (by 3% or 218,331 pixels) by nearly the equivalent amount in the Equateur wetlands map (Table 3.2).

A second, though comparatively minor, explanation is that the Equateur method does not allow floodplain to exist as an isolated area inside an upland

region. This is based on the reasoning that floodplain is an environment continuous with running water bodies. It is for this reason that the upland rule implies that no upland object may overlap with the HydroSHEDS River vector. In the Africover map, however, there are several instances where secondary floodplain appears to be cut off from the primary floodplain, which would also cause the Equateur method to produce comparatively less upland and more floodplain (Figure 3.1). These “cut offs” do not necessarily mean that there is no hydrologic connectivity between the secondary and primary floodplains, but rather that the floodplain was not discernible from the LANDSAT imagery (e.g., in the case of a narrow gorge).

Finally, although the minimum mapping area is smaller for Africover (34 ha vs. 50 ha), the Equateur map exhibits many small upland areas along all river courses where Africover shows none (Figure 3.1). The heightened sensitivity to upland of this method would slightly increase the quantity of upland compared to the less-sensitive Africover method, which uses only optical data (and thus the spectral reflectance of vegetation canopy) to derive landcover classes. As De Grandi et al. (2000a) and Mayaux et al. (2000) note, the visual interpretation of satellite imagery tends to eliminate small and narrow features, and this is likely responsible for the difference.

3.1.3 Lake

Of all classifications, producer's and user's accuracies are highest for lake at 96% and 97% respectively (Table 3.1). Most of the omission error is explained by confusion with flooded forest (46%), herbaceous (22%) and nonflooded forest (18%). Most of the commission error is explained by confusion with upland (47%) and forest (33%). In terms of quantification, the Equateur lake class closely matches the Africover lake class, underestimating it by 2% (Table 3.2).

The lake classification is both well quantified and located. This is not surprising given the ease of identifying open water with both optical and radar data and the accuracy of the SWBD ancillary dataset, whose overlap with open water objects serves as the primary rule for this class. The extent of lake area is slightly less in the Equateur wetlands map which may be a consequence of greater flooding during the Africover imagery acquisition compared to the timing of the SRTM data collection. Overall, the lake class is very well represented in this method.

3.1.4 River

Producer's and user's accuracies are similar for the river class at 84% and 79% respectively (Table 3.1). The omission error is composed of confusion with forest (71%) and nonflooded forest (13%). Commission errors are split among all of the vegetated classes: forest (32%), upland (23%), woodland (20%), shrub

(14%), and herbaceous (11%). Compared to Africover, the quantity of the Equateur river class approximates well, overestimating by 5% (Table 3.2).

This over-quantification may be the result of the greater sensitivity of radar to rivers than optical sensors, particularly as L-HH radar is capable of penetrating vegetation canopies that may otherwise hide shorelines in optical imagery. This could also be explained by the tendency of eliminating small (or in this case, narrow) features during the visual interpretation of Africover. River overestimation may also be the consequence of differences in objectivity and consistency between the methods of map making. The multi-resolution and spectral segmentation procedures identify small, spectrally distinct objects objectively. The Busira River, for example, terminates earlier in the Africover dataset compared to the Equateur map. Compare this to the relatively early termination of the Lopori and Maringa Rivers (Figure 3.1). This can explain the commission errors of river with the flooded vegetation classes. Generally, the river class is well classified without significant quantification or location error.

3.1.5 Floodplain Shrub

Of all classifications, producer's accuracy is lowest for shrub at 13%, with a user's accuracy of 85% (Table 3.1). Most of the omission error is confusion with flooded forest (35%), herbaceous (30%), and nonflooded forest (26%). Most of the commission error is confusion with upland (49%), forest (30%), and

herbaceous (15%). In terms of quantification, 84% less shrub is quantified by the Equateur method compared to Africover (Table 3.2).

The clearest example of shrub underestimation occurs on the left bank of the Congo River as it enters the area in the north and along the left shoreline further south (Figure 3.1). There is also considerable confusion with herbaceous vegetation for shrub along the Giri River and on the left bank of the Congo River where it exits the Equateur district (Figure 3.1). The Giri River is well known to show complex mosaics of flooded herbaceous and shrub vegetation (Hughes et al. 1992, Mayaux et al. 2002). It also is the most accurate in terms of the low- and high-water mosaics representing true low- and high-water conditions (Rosenqvist and Birkett 2002). Therefore, the unidirectional change in stage assumed during the development of the Hess et al. (2003) parallel-piped classifier holds truest for this river and, when corroborated with the Directory of African Wetlands and a previous wetland map of the region (Mayaux et al. 2002), is likely more representative of ground truth than Africover. The other areas of shrub vegetation cannot be verified. Visually, the shrub class of Africover tends to coincide with the shrub and herbaceous classes of the Equateur map, except for the large patch near Bolombo (Figure 3.1).

3.1.6 Floodplain Herbaceous Vegetation

Producer's accuracy is 20% and user's accuracy is 6% for the herbaceous class (Table 3.1). The error associated with the low producer's accuracy comes from confusion with flooded forest (38%), nonflooded forest (30%), and river (21%). The commission error is explained mostly by confusion with shrub (49%) and upland (37%). The Equateur method over-quantifies herbaceous cover by 259% or approximately 112,000 pixels; the largest quantification discrepancy (Table 3.2).

The majority of the shrub confusion occurs along the Giri River, which is known to contain mostly herbaceous vegetation, both rooted and floating (Hughes et al. 1992, De Grandi et al. 2000a). Large sedges also occur along the Giri, and it is well documented that emergent herbaceous vegetation greater than 1.5 m in height can be mistaken for shrub in L-band frequencies (Silva et al. 2008), and that interpretation of such vegetation from LANDSAT imagery is often confused for shrub as well. It is possible that this can also explain the confusion between flooded herbaceous and shrub on the southern left bank of the Congo River, but no documentation exists to confirm this. It is important to note that where Africover indicates flooded herbaceous (e.g., north of the confluence of the Ruki River with the Congo River and along the right bank of the Congo in the northern reach), the Equateur method also shows flooded herbaceous vegetation

(Figure 3.1). Therefore, it is reasonable to assume that the method presented here better represents flooded herbaceous vegetation than Africover, especially along the Giri River.

3.2 Simplified Wetlands Map

The simplified wetlands map includes five classes: upland, lake, river, tall vegetation and short vegetation. The tall vegetation class is the combination of the flooded floodplain forest and nonflooded floodplain forest classes. The short vegetation class is the combination of the floodplain shrub and herbaceous vegetation classes. The simplified wetlands map and corresponding Africover map are shown in Figure 3.2.

Strategically collapsing the classes from seven to five increased the overall accuracy from 47% to 76% and doubled the KIA from 28% to 57% (Table 3.3). All of the classes were well quantified except short vegetation, which was underestimated by 38% (Table 3.4).

3.2.1 Tall Floodplain Vegetation

The tall vegetation class combines both the floodplain forest and woodland classes to effectively become a flooded trees class. The producer's and user's accuracies are 80% and 76% respectively (Table 3.3). Nearly all of the omission and commission error is with upland at 96% and 86% respectively. Compared to

Africover, the tall vegetation class is well quantified with 6% difference (Table 3.4).

3.2.2 Short Floodplain Vegetation

The short vegetation class collapses the shrub and herbaceous classes of the full wetland map into a single class. The producer's and user's accuracies are 37% and 60% respectively (Table 3.3). Most of the producer's error is explained by confusion with tall vegetation (84%), and user's error is associated with confusion with upland (72%) and tall vegetation (22%). Quantification of short vegetation by the Equateur method is 38% less than indicated by the corresponding Africover class (Table. 3.4).

The shrub and herbaceous classes which make up the short vegetation class remain difficult to correspond with Africover. L-HH is well known to be most sensitive to flooded forest with decreasing sensitivity to shrub and herbaceous vegetation (Hess et al. 2003). This may explain the confusion between the two classes, but not its confusion with the tall vegetation class.

Table 3.3: Error matrix and accuracy measures for the simplified wetlands map, in hectares.

		Reference Data					Classified
		U	L	R	TV	SV	Total
Classified Data	U	**3,432,894**	344	3,215	972,367	13,044	4,421,863
	L	957	**75,316**	0	683	409	77,365
	R	13,244	119	**221,049**	29,680	14,328	278,420
	TV	1,125,238	2,144	36,525	**4,062,521**	146,119	5,372,546
	SV	49,000	777	3,459	14,934	**102,248**	170,418
Reference Total		4,621,333	78,699	264,247	5,080,185	276,148	**10,320,612**

		Producer's Accuracy	User's Accuracy		
U	= Upland	74%	78%		
L	= Lake	96%	97%		
R	= River	84%	79%		
TV	= Tall veg.	80%	76%	Overall Accuracy	**76%**
SV	= Short veg.	37%	60%	KIA	**57%**

Table 3.4: Comparison of quantity between the mapped and reference simplified wetland classes.

Class	Mapped ha (M)	Reference ha (R)	Difference (D = M - R)	% Difference (%=D/R*100)
Upland	4,421,863	4,621,333	-199,470	**-4**
Lake	77,365	78,699	-1,334	**-2**
River	278,420	264,247	14,173	**5**
Tall vegetation	5,372,546	5,080,185	292,361	**6**
Short vegetation	170,418	276,148	-105,730	**-38**

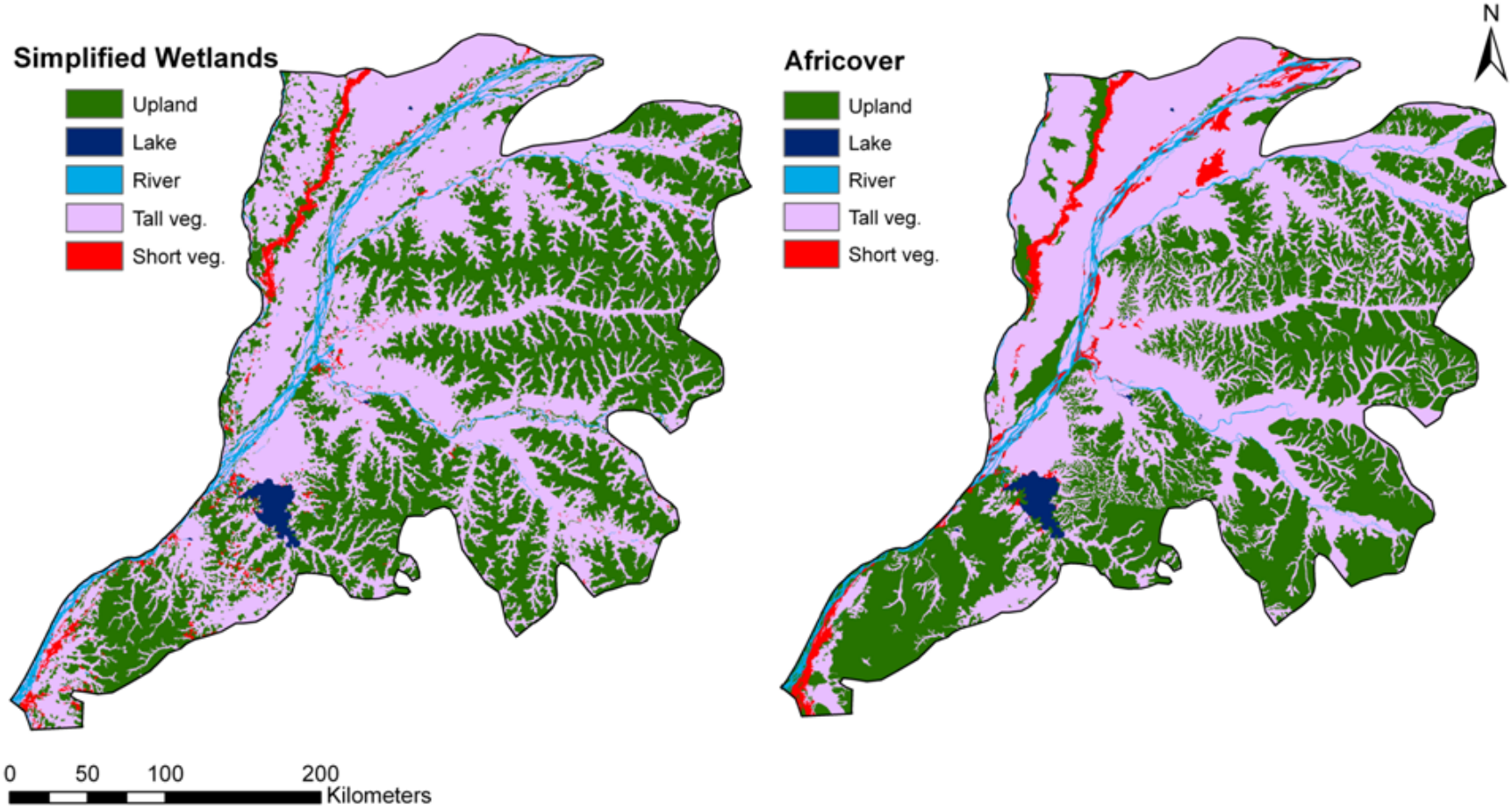

Figure 3.2: A visual comparison of the simplified wetlands map and the reclassified Africover reference map.

3.3 Basic Floodplain Map

The basic floodplain map includes three classes: upland, open water and floodplain. The open water class is a combination of the lake and river classes, and the floodplain class is a combination of tall and short vegetation classes from the simplified wetlands map. The basic floodplain map and corresponding Africover map are shown in Figure 3.3.

The overall accuracy of the basic floodplain map, compared to Africover, is 78% with a KIA of 59% (Table 3.5). Since quantification is generally comparable for all classes between the Equateur and Africover wetland mask maps (Table 3.6), most of the error is related to location.

3.3.1 Open Water

The open water class more closely corresponds to Africover's open water class with producer's and user's accuracies of 86% and 83% respectively (Table 3.5). Most of the error is confusion with the floodplain environment, which explains 92% of omission error and 76% of commission error. This is expected given that floodplain by definition borders open water. The difference in quantity of open water in the Equateur and Africover maps is small, with 4% more open water in the Equateur map (Table 3.6).

Table 3.5: Error matrix and accuracy measures for the basic floodplain map, in hectares.

		Reference Data			Classified Total
		U	OW	FP	
Classified Data	U	**3,432,894**	3,559	985,411	4,421,863
	OW	14,201	**296,483**	45,101	355,785
	FP	1,174,238	42,905	**4,325,822**	5,542,965
Reference Total		4,621,333	342,946	5,356,333	**10,320,612**

		Producer's Accuracy	User's Accuracy		
U	= Upland	74%	78%		
OW	= Open water	86%	83%	Overall Accuracy	**78%**
FP	= Floodplain	81%	78%	KIA	**59%**

Table 3.6 Comparison of quantity between the mapped and reference basic floodplain classes.

Class	Mapped ha (M)	Reference ha (R)	Difference (D = M - R)	% Difference (%=D/R*100)
Upland	4,421,863	4,621,333	-199,470	**-4**
Open water	355,785	342,946	12,838	**4**
Floodplain	5,542,965	5,356,333	186,631	**3**

3.3.2 Floodplain

The floodplain class represents all areas that are neither upland nor open water. The producer's and user's accuracies are high at 81% and 78% respectively (Table 3.5). The primary source of confusion from a producer's and user's perspective is with upland at 96% of the error for each. This can be explained by the discussion of upland discrepancies above, where upland is underestimated compared to Africover. Therefore, the floodplain environment will be overestimated by a similar amount (Table 3.6). Quantification of the floodplain environment is slightly closer to the quantity specified by Africover than upland or open water with 3% more floodplain area in the Equateur map (Table 3.6).

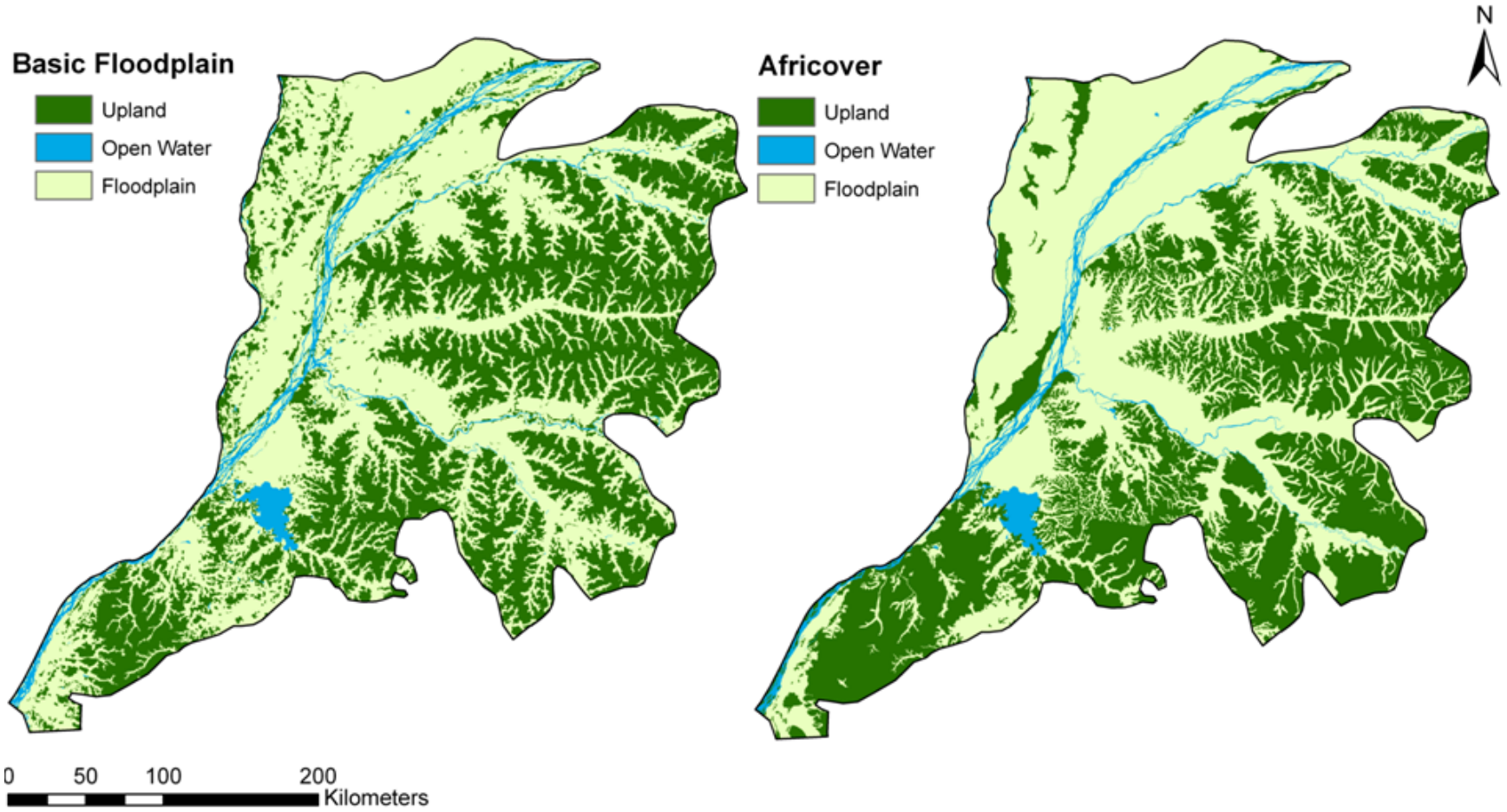

Figure 3.3: A visual comparison of the basic floodplain map and the reclassified Africover reference map.

4. General Discussion and Conclusions

4.1 Simplified Wetlands and Basic Floodplain Maps: Comparison to Africover

While the comparison to Africover as a measure of accuracy is not robust and could be, without explanation, misleading, it provides a structure to assess discrepancies between the maps, and highlights the pitfalls of comparing maps derived using different source data and methods.

Similar overall accuracies and KIAs for both the simple wetlands map and basic floodplain map indicate that the mapping method for these levels have achieved maximum correspondence with Africover (Figure 4.1). Africover has only demonstrated 60% accuracy at the termination of the first phase of classification, so the purpose of these comparisons is not to replicate Africover but to use it as an indicator of map quality. Therefore, it is reasonable to assume that the simplified wetlands and floodplain maps are at least comparable to Africover in accuracy given that the errors found in the Equateur maps are corroborated by other sources (Hughes et al. 1992, De Grandi et al. 2000a, Mayaux et al. 2002).

Given the different source data, classification methods, and the questionable accuracy of Africover, the similarity in quantification and overall accuracies and KIAs of the classes of both the simplified wetlands and floodplain maps indicate that this method is successful as a rapid method of tropical

floodplain wetland classification at these levels of classification. This is possible because the L-HH radar and topography datasets are more sensitive to and consistent with the physiognomic-hydrologic wetland classification scheme used, and because the object-oriented segmentation and classification is a more objective, semi-automated, and consistent approach to image analysis than visual interpretation.

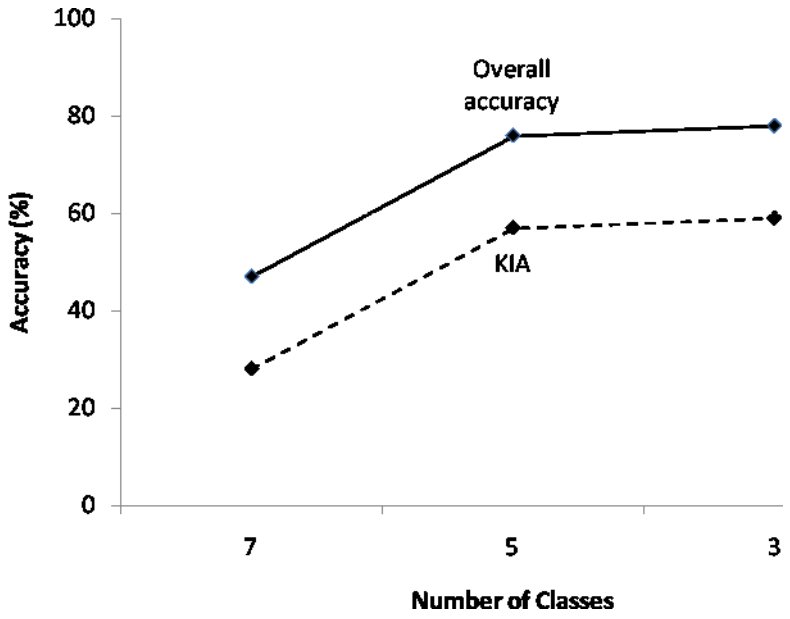

Figure 4.1: Accuracy obtained using Africover as reference data for the three levels of wetland class aggregation.

4.2 Simplified Wetlands and Basic Floodplain Maps: Comparison to other maps

Further, though qualitative, insight to the quality of these maps is gained from the visual comparisons of the simple wetlands and floodplain maps to leading, similar maps of the region.

De Grandi et al. (2000a) produced a map based on C-VV that arrived at a very similar distribution of floodplains as the basic floodplain map (Figure 4.2). The central-basin-wide map shows similar thematic classes with comparable overall accuracy of 71% against a LANDSAT-derived forest inventory map (SPIAF 1995). De Grandi et al. (2000a) did not present a measure of KIA. However, when comparing producer's and user's accuracies for floodplain ("swamp forest" in De Grandi et al. [2000a]), correspondence is much higher at 81% and 78% respectively, versus 67% and 53% found by De Grandi et al. (2000a). Visually, the basic floodplain map tends to show more floodplain compared to De Grandi et al. (2000a), but shows a similar pattern of upland, particularly along the Oubangui, Giri and Congo River courses (Figure 4.2).

The distribution of upland is similar in the most thematically detailed wetland map of the central Congo basin, which was derived from combining one mosaic of C-VV radar with L-HH radar (Figure 4.3). Swamp grassland, permanently flooded forest, and periodically flooded forest are mapped in Mayaux et al. (2002). Swamp grassland is analogous to the short vegetation class of the simplified wetlands map, and appears disjointed and with less total quantity compared to the simple wetlands map (Figure 4.3). Within the Equateur Province, Mayaux et al. (2002) indicate that swamp grassland only occurs along the Giri River, which is in disagreement with the simplified and full wetlands map

presented here, as well as with Africover (e.g., see areas by Yumbi in the southwest, around Lake Tumba, and north of Mbandaka). The periodically flooded forest and permanently flooded forest classes match well with the nonflooded and flooded floodplain forest in the full Equateur wetlands map. Only between the Oubangui and Giri Rivers in the north is there significant regional difference between the two: the Equateur map indicates periodically flooded forest where Mayaux et al. (2002) indicate lowland rain forest (i.e., upland). Similar to De Grandi et al. (2000a), the Equateur map appears to exceed the nonflooded floodplain forest class at the expense of upland in comparison to Mayaux et al. (2002).

A more quantitative comparison between the simplified wetlands map and the map of Mayaux et al. (2002) shows producer's accuracies for lowland rain forest, swamp forest, swamp grassland and water to be 87%, 59%, 80%, and 80% respectively compared to the 74%, 80%, 37%, and 86% for corresponding classes (upland, tall vegetation, short vegetation, and open water) in the wetlands map of Figure 4.2. User's accuracies for the same classes were 75%, 72%, 80%, and 86% compared to the 78%, 76%, 60%, and 83% of the Equateur method. Both maps have comparable overall, producer's and user's accuracies compared to their reference maps. As in this study, both reference maps were derived from visually interpreted LANDSAT imagery with different sensitivities

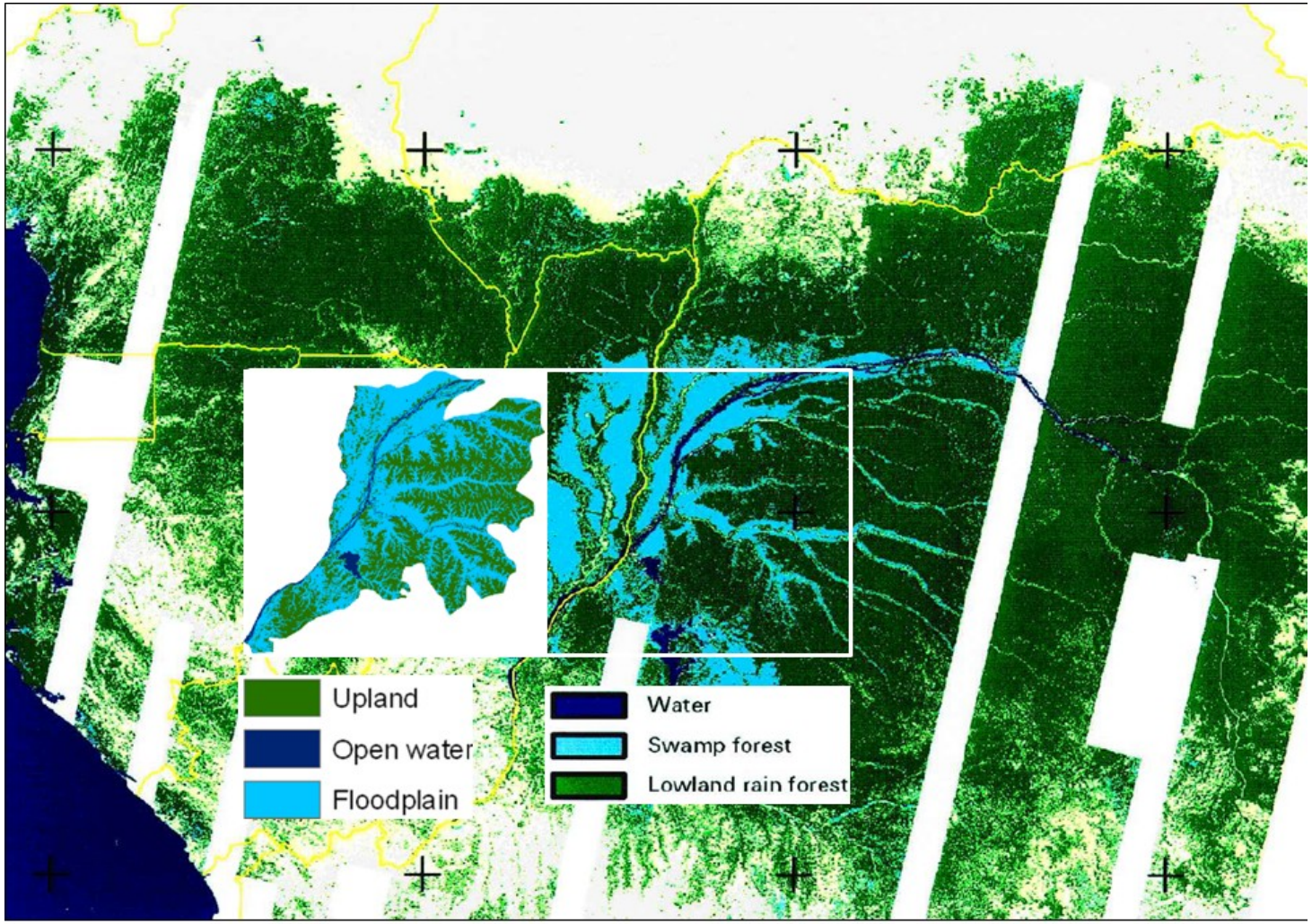

Figure 4.2: Basic Equateur floodplain map (inserted left) and the leading wetland map of the central Congo River basin: De Grandi et al. (2000a). Notice the close correspondence between Equateur upland and lowland rain forest, and Equateur floodplain and swamp forest.

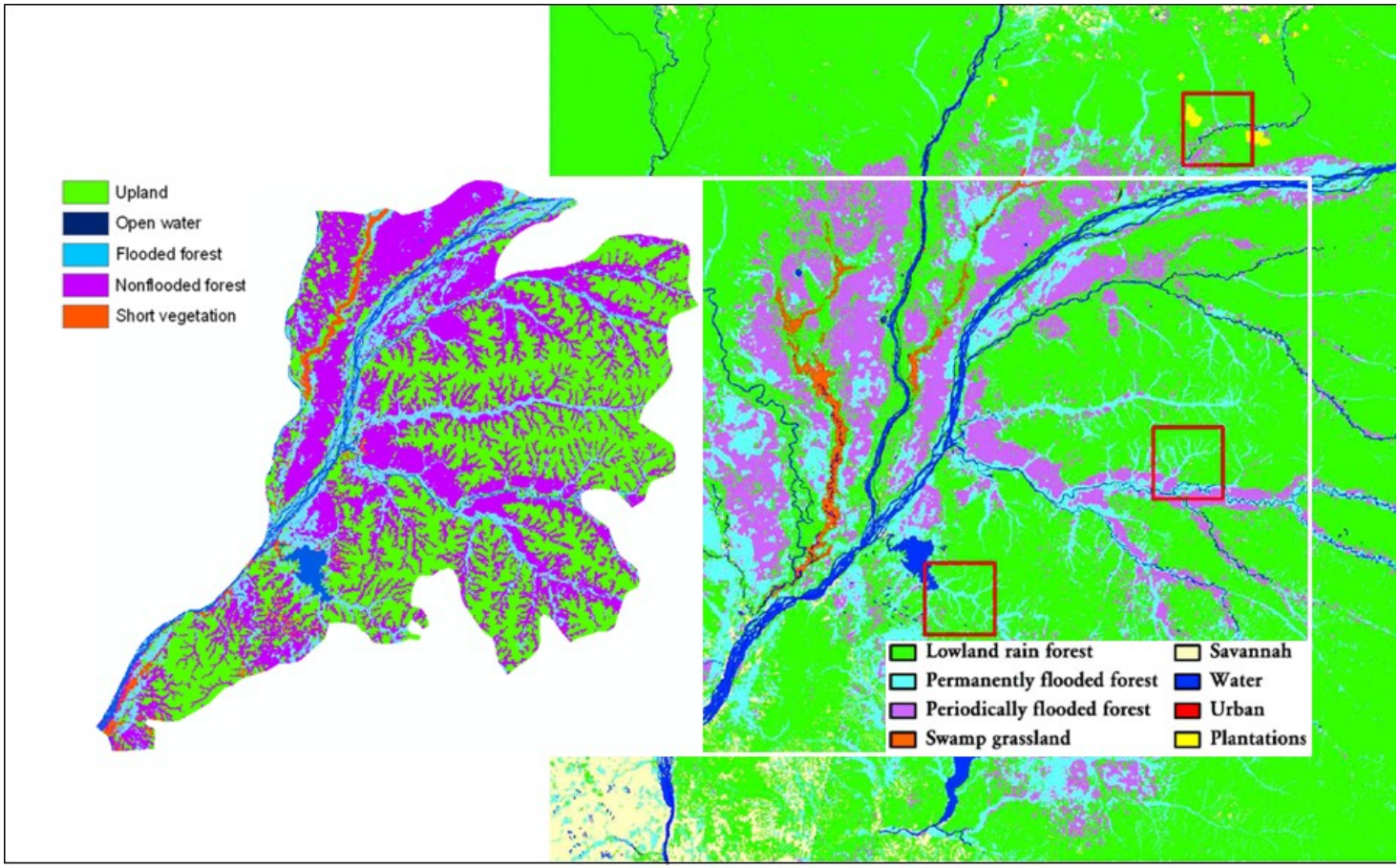

Figure 4.3: Simplified Equateur wetlands map (left) and the leading wetland map of the Equateur region: Mayaux et al. (2002). Notice the close correspondence between Equateur flooded forest and permanently flooded forest, Equateur nonflooded forest and periodically flooded forest, and Equateur short vegetation with swamp grassland.

that suggest that discrepancies are actually improvements over their respective reference maps (Mayaux et al. 2002). With the exception of overestimating the area of floodplain, the Equateur method appears to approximate the classes of the leading wetland maps of the region well, and may produce a more accurate short vegetation class.

4.3 Full Equateur Wetlands Map

The Equateur method is also useful for providing additional classes previously unmapped in the region, distinguishing between shrub and herbaceous vegetation. However, the accuracy of these classes can only currently be verified by the single available high-resolution landcover map of the region: Africover. As indicated in the results presented above, the distribution of shrub and herbaceous vegetation between the Equateur and Africover maps is similar. The Equateur map shows considerably more herbaceous vegetation where Africover indicates shrub, particularly along the Giri River, but other descriptive and mapping sources support the results of the Equateur map. This, in addition to the visual comparison of the flooded floodplain forest, nonflooded floodplain forest, and short vegetation classes to Mayaux et al. (2002) above, indicates that the accuracy of the full Equateur wetlands map is higher than indicated by its comparison to Africover, but it is unknown to what degree.

An interesting failure of the classification scheme was to correctly identify floodplain woodland. This class was adapted directly from the parallel-piped classifier derived in Hess et al. (2003) from the PDF of flooded woodland found from training samples in the central Amazon. When comparing the distributions of classes to the map of Mayaux et al. (2002), it is evident that the flooded woodland classifier of Hess et al. (2003) represents nonflooded forest in the full Equateur wetlands map. Since L-HH is sensitive to volumetric scattering in the canopy (increasing backscatter with denser canopy) and to flooded, vegetated surfaces via a double-bounce mechanism, it is possible that the dual-mosaic response of the flooded woodland in the central Amazon (high double bounce return, lower volumetric scattering) approximates that of nonflooded forest in the central Congo (low double bounce return, higher volumetric scattering). This is supported by a comparison of the PDFs illustrated in Hess et al. (2003), which shows the flooded woodland class PDF entirely overlapping and peaking similarly to the narrower nonflooded forest class PDF (Figure 4.4).

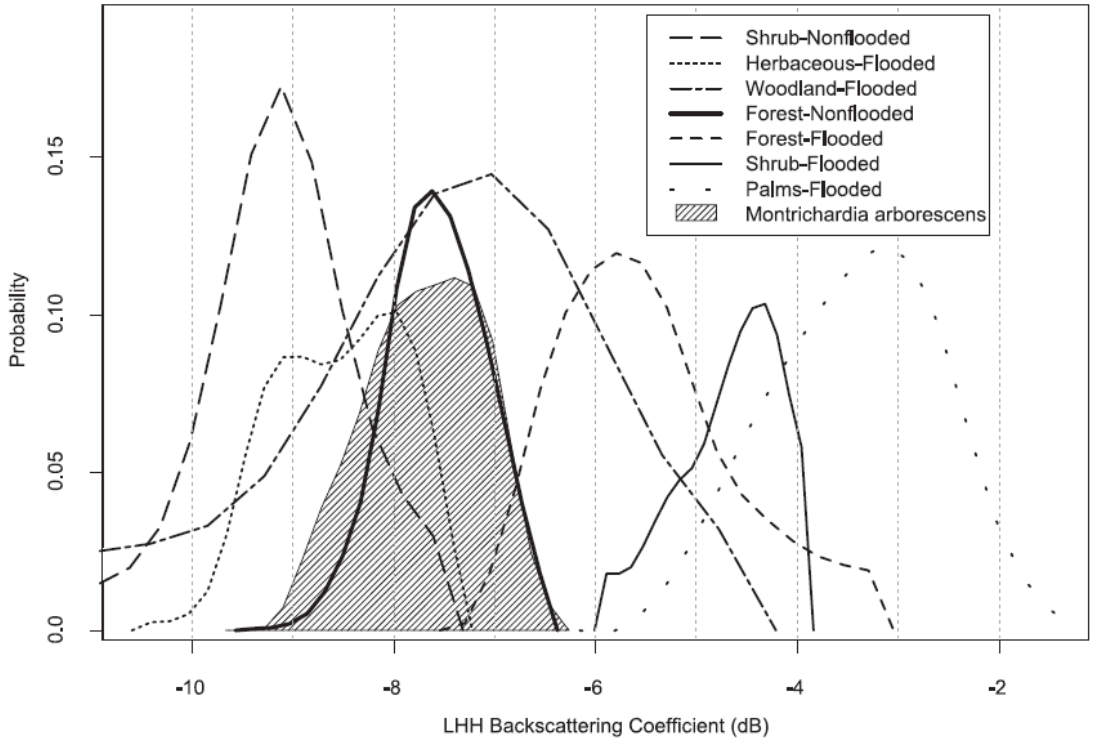

Figure 4.4: A comparison of probability density functions derived from training sites in the central Amazon and used to determine the parallel-piped classifier thresholds of Hess et al. (2003). Notice the overlap between the woodland-flooded and forest-nonflooded classes. From Hess et al. (2003).

4.4 New Insights

Of the 100,000 km^2 of Equateur, approximately 40,000 km^2 qualify as floodplain wetland. No previous estimates of wetland extent have been published for this specific area, but Hughes et al. (1992) suggest a conservative 120,000 km^2 of permanently or seasonally inundated forest in the D. R. Congo portion of the central Congo basin and a further 65,000 km^2 in the Republic of Congo portion, for a total of 185,000 km^2. If the same proportion of land at the same elevation as Equateur (255 to 455 m) in the Congo basin (820,000 km^2) is

assumed wetland—which, given Equateur's central location, makes this a maximum estimate of wetlands in the central basin—then approximately 330,000 km^2 of wetlands could be calculated as the maximum wetland area for the central Congo basin. This estimate is much higher than given by the conservative estimate in Hughes et al. (1992). Therefore, it is hypothesized here that at least 185,000 km^2 and no more than 330,000 km^2 of wetlands exist in the central Congo basin. In terms of wetland distribution, the results are visually comparable to the most detailed wetland assessment of the area, although the floodplain nonflooded forest of the Equateur map is generous compared to previous maps (Figures 4.2 and 4.3), indicating that the total amount of wetlands in the central basin is closer to the 185,000 km^2 proposed by Hughes et al. (1992).

More importantly, the Equateur method provides more classes and a rapid method of reassessing wetland quantity and distribution than any available method for the region. Large-scale hydrological models do not currently include aquatic vegetation in their calculations, which is important in determining floodwave attenuation as well as evapotranspiration fluxes. This study has also produced vegetation classes of interest to carbon modelers but still requires their seasonal flooding dynamics for incorporation into carbon models. Rosenqvist and Birkett (2002) indicate that high-water conditions are captured fairly well in this region, therefore, the results shown here can be taken as a first estimate of

maximum wetland extent for Equateur. Although flooding dynamics are not captured in this study, it is not a limitation of the method but rather of the datasets. Upon further releases of L-band datasets for the region, this method could be expanded to include the full physiognomic-hydrologic classifications used in Hess et al. (2003). The seasonal wetland distribution information that would result can be used in conjunction with field measurements of methane emissions, as calculated for the Amazon by Melack et al. (2004). The same information on the type and distribution of wetlands illustrated in this study can be used for fishery management, as fishing is a major source of protein and economic activity in the region. However, one wetland class that these data could not resolve that is important to ecological and cultural welfare is *Raphia* palms. It is well documented that *Raphia* spp. (a cosmopolitan wetland palm) is the primary habitat of the otherwise little studied and endemic lowland gorilla, in addition to significant food and cultural value (grubs, wine) to the local Bantu and Pygmy peoples (Hart and Hart 1986). Africover includes a custom *Raphia* spp. class in the D. R. Congo dataset, and these polygon outlines were used for training to identify other floodplain objects that qualified as *Raphia* spp. The radar backscatter was not distinguishable from nonflooded floodplain forest, and was left out of the classification. In this case, optical imagery would be of use in capturing this special class, as was successfully done by Hamilton et al. (2007)

using LANDSAT imagery in conjunction with radar and elevation data over the Madre de Dios subbasin of the Amazon River basin. It is also possible that the multi-polarized radar imagery now made available by the ALOS/PALSAR satellite could also distinguish this class, however, no study has yet determined this.

4.5 Limitations and Future Work

A clear limitation of this method is the availability of dual-season L-HH datasets. The radar datasets used here exist—though only in dual-season form for the Amazon and the Congo—for the rest of the tropics. Dual-season L-HH mosaics were essential for distinguishing the flooded shrub and herbaceous vegetation classes. With single-season L-HH data, only flooded and nonflooded forest wetland classes could be reliably classified. The multipolarized ALOS/PALSAR L-band sensor has since succeeded the JERS-1/SAR L-HH sensor, and currently releases 500 m mosaics of the African continent every cycle, or 46 days. In addition, a new radar dataset based on ALOS/PALSAR consisting of 50 m resolution, orthorectified mosaics is soon to be released from the EC JRC with the objective of capturing low- and high-water conditions over the Congo basin.

However, even with well-timed L-band radar mosaics, Hess et al. (2003) found that their classifier did not perform well in tidally inundated areas, interfluvial white-sand wetlands with low biomass shrubs and sedges, and in

wetlands within large savannas where there is low-biomass and the herbaceous vegetation is rooted and emergent rather than high-biomass and floating. The Congo River has little tidally inundated area at its mouth but does exhibit extensive savannas to the north and south of the central basin. Important, large wetland systems lie in the southern portion of the basin such as in the Kamolondo Depression, where the Upemba Lakes and approximately 800,000 ha of forested and herbaceous wetlands occur (Hughes et al. 1992). Therefore, the data and classifier presented here—though simpler than that used in Hess et al. (2003)—may require changes to adapt to the vegetation and geomorphology of different regions and (or) to capture important classes not included in this wetland scheme.

Perhaps the most beneficial additional information would be an optical dataset, which could further distinguish forest types and include species-specific classifications such as *Raphia* spp. palms, which were indistinguishable from flooded forest in Hess et al. (2003) and from nonflooded floodplain forest in this study. Hamilton et al. (2007), for example, were successful identifying a *Raphia* spp. palm class in a sub-basin classification of the Amazon using LANDSAT/ETM+ imagery. Although the problem of cloud cover precludes optical imagery from being the principle source of rapid tropical floodplain wetland mapping method, the recent availability of optical, 300 m resolution

global composites from the MERIS/Globcover initiative could serve as a complimentary dataset in future, large-scale wetland mapping studies, especially as the multipolarized C-band ENVISAT/ASAR sensor is also employed in this initiative to delineate wetland from humid tropical forests.

C-band radar data would also provide complimentary information by improving the distinction between the herbaceous and shrub classes, since these vegetation covers are difficult to distinguish between in the L-band wavelength. Simard et al. (2002), for example, found that merging L-HH and C-VV data could effectively map woody and herbaceous wetlands along the coast of Gabon. The recent release of 150 m resolution C-band mosaics from the ENVISAT/ASAR program could be incorporated to improve the accuracy of the short vegetation classes of this method and to potentially make further differentiations between forest types based on canopy backscatter signatures or texture.

The TERRA/ASTER 30 m global DEM was recently released for public use, and exceeds the HydroSHEDS DEM in spatial resolution with approximately the same accuracy (ASTER 2009). With a higher resolution DEM, sinuous meader scrolls and smaller channel bars common to the floodplain environment of large rivers could be detected. These objects could then be distinguished from upland based on proximity to river and length-to-width ratios, for example.

4.6 Conclusions

This study has achieved a rapid method of tropical floodplain classification comparable in thematic detail to the leading wetland map of the central Congo basin (Mayaux et al. 2002) and in accuracy to the only publicly available, high resolution wetland map of the region: Africover. It also provides a limit of maximum wetland area in the central Congo basin and a first estimate of floodplain shrub and herbaceous vegetation classes in the Equateur administrative region. The method demonstrates the power of integrating several wetland-relevant, digital datasets, and indicates that the parallel-piped classifier derived from Hess et al. (2003) is valid for use in the central Congo basin with the exception of confusing nonflooded floodplain forest for flooded woodland. The addition of elevation and slope datasets and the HydroSHEDS Rivers vector layer reduced the reliance on L-HH radar for the upland class, since it was found that backscatter of upland overlapped with forest and herbaceous cover in the parallel-piped classifier of Hess et al. (2003). The addition of the SWBD Lakes dataset enabled the distinction of lakes from rivers. In addition, the study provides further evidence that image segmentation is both a practical and effective method for large raster dataset analysis (Costa et al. 2002, Hess et al. 2003, Durieux et al. 2007).

There are several advantages to the object-oriented approach employed in this study: the ability to incorporate other datasets in a transparent way (via the process tree) without complex image fusion procedures involved with traditional pixel classifications. This capability allows the method to be customized or improved upon with the growing number of global and near-global digital datasets relevant to wetland mapping. The object-oriented approach is also unbiased compared to visual interpretation and manual delineation of satellite imagery (e.g., Africover).

There are limitations, however, since classification rules will likely need to be adapted to different geomorphological and ecological settings outside of the central basin. Also, the scale parameters reported here do not refer to any known algorithm, only to the scale factor unique to the image analysis software used in this study. Therefore, it is unknown how the data are actually treated to create image objects of the appropriate size and shape. Lastly, dual-season radar data are necessary to determine shrub and herbaceous vegetation from L-HH radar. However, adding C-band radar or potentially multi-polarized L-band data may provide enough information to better distinguish these classes. Greater availability of high-resolution, large scale optical composites may also improve classification accuracy and would also provide more ecologically important wetland classes such as *Raphia* spp. palm stands.

As no extensive fieldwork has been conducted to verify Africover, the accuracy of this method cannot be ascertained, though it is comparable to previous maps of the region. While computer classification of remote sensing data should never supersede field observations and data, their outputs can be used to improve hydrological and biogeochemical models, in addition to affecting science-based conservation strategies that are urgently needed in many rapidly developing tropical countries such as the D. R. Congo that depend upon many floodplain wetland ecosystem services (Thieme et al. 2007).

A rapid method of tropical floodplain wetland mapping over a large area of the central Congo floodplain has been produced with relevance to hydrologists, biogeochemists, and conservationists that is comparable to the thematic detail and accuracy of previous work in addition to providing two new classes of wide interest: floodplain shrub and herbaceous vegetation. Africover is the only dataset with comparable spatial and thematic detail; however, it suffers from a dependency on cloud-free imagery that makes it difficult to acquire multi-temporal imagery from different seasons, in addition to an inability to penetrate dense tropical canopies to determine flood extent. Thematic detail is improved with the Equateur method in comparison with Africover with better discrimination between the shrub and herbaceous classes. The semi-automated nature of the Equateur method also makes for a consistent and rapid method of monitoring

wetland classes in comparison to the interpretation of LANDSAT imagery used in Africover. Finally, this study highlights the potential of wide area, high-resolution L-HH radar and topography datasets for mapping tropical floodplain wetlands at an appropriate scale for regional inventory and monitoring purposes, and can be further improved by the growing availability of relevant, digital datasets and their consistent, semi-automatic integration in an object-oriented analysis.

References

ASTER (2009). Features of ASTER DEM. Online at http://www.ersdac.or.jp/GDEM/E/2.html

Ausseil, A., Dymond, J., & Shepherd, J. (2007). Rapid mapping and prioritisation of wetland sites in the Manawatu–Wanganui region, New Zealand. *Environmental Management, 39*, 316-325

Baker, C., Lawrence, R., Montague, C., & Patten, D. (2006). Mapping wetlands and riparian areas using Landsat ETM+ imagery and decision-tree-based models. *Wetlands, 26*, 465-474

Blake, S., Rogers, E., Fay, J., Ngangoue, M., & Ebeke, G. (1995). Swamp gorillas in northern Congo. *African Journal of Ecology, 33*, 285-290

Bolstad, P. V. & Lillesand, T. M. (1992). Rule-based classification models – flexible integration of satellite imagery and thematic spatial data. *Photogrammetric Engineering and Remote Sensing, 58*, 965-971

Bultot, F. (1971). *Atlas climatique du basin congolaise, vol. 3, température et humidité de l'air, rosée, température du sol.* Bruxelles, Belgium: Institut National pour l'Etude Agronomique au Congo.

Campbell, D. (2005) The Congo River basin. In Fraser, L. H. & Keddy, P. A. (Eds.), *The world's largest wetlands*. (pp. 149–165). Cambridge, UK: University Press.

CCRS (Canadian Centre for Remote Sensing) (2007). Resolution, polarization, and imaging. Online at http://www.space.gc.ca/asc/eng/satellites/radarsat2/inf_data.asp

CCRS (Canadian Centre for Remote Sensing) (2009). Glossary of remote sensing terms. Online at http://www.ccrs.nrcan.gc.ca/glossary/index_e.php?Id=2980

Chen, Y., & Prinn, R. (2006). Estimation of atmospheric methane emissions between 1996 and 2001 using a three-dimensional global chemical transport model. *Journal of Geophysical Research-Atmospheres, 111*, D10307

Congalton, R. G., & Green, K. (2009). Assessing the accuracy of remotely sensed data: Principles and practices. Second edition. Boca Raton: CRC Press.

Costa, M. (2004). Use of SAR satellites for mapping zonation of vegetation communities in the Amazon floodplain. *International Journal of Remote Sensing, 25*, 1817-1835

Costa, M., Niemann, O., Novo, E., & Ahern, F. (2002). Biophysical properties and mapping of aquatic vegetation during the hydrological cycle of the Amazon floodplain using JERS-1 and RADARSAT. *International Journal of Remote Sensing, 23*, 1401-1426

Costa, M., & Telmer, K. (2007). Mapping and monitoring lakes in the Brazilian Pantanal wetland using synthetic aperture radar imagery. *Aquatic Conservation: Marine and Freshwater Ecosystems, 17*

Constanza, R., Darge, R., Degroot, R., Farber, S., Grasso, M., Hannon, B., Limburg, K., Naeem, S., Oneill, R. V., Paruelo, J., Raskin, R. G., Sutton, P. & Vandenbelt, M. (1997). The value of the world's ecosystem services and natural capital. *Nature, 387*, 253-260

Coughanowr, C. (1998). Wetlands of the humid tropics. *IHP humid tropics programme series, 12*

Coynel, A., Seyler, P., Etcheber, H., Meybeck, M., & Orange, D. (2005). Spatial and seasonal dynamics of total suspended sediment and organic carbon species in the Congo River. *Global Biogeochemical Cycles, 19,* 17

Daniels, A. (2006). Incorporating domain knowledge and spatial relationships into land cover classifications: a rule-based approach. *International Journal of Remote Sensing, 27*, 2949-2975

Davidson, N., & Finlayson, C. (2007). Earth Observation for wetland inventory, assessment and monitoring. *Aquatic Conservation: Marine and Freshwater Ecosystems, 17*

De Grandi, G., Mayaux, P., Malingreau, J., Rosenqvist, A., Saatchi, S., & Simard, M. (2000a). New perspectives on global ecosystems from wide-area radar mosaics: flooded forest mapping in the tropics. *International Journal of Remote Sensing, 21*, 1235-1249

De Grandi, G., Mayaux, P., Rauste, Y., Rosenqvist, A., Simard, M., & Saatchi, S. (2000b). The Global Rain Forest Mapping Project JERS-1 radar mosaic of tropical Africa: development and product characterization aspects. *IEEE Transactions on Geoscience and Remote Sensing, 38*, 2218-2233

Devol, A. H., Richey, J. E., Forsberg, B. R., & Martinelli, L. A. (1990). Seasonal dynamics in methane emissions from the Amazon River floodplain to the troposphere. *Journal of Geophysical Research, 95(10)*, 16,417-16,426

Di Gregorio, A., & Jansen, L. (2005). *Land Cover Classification System, Classification Concepts and User Manual.* Food and Agriculture Organization of the United Nations, Viale delle Terme di Caracalla, Rome, Italy.

Dugan, P. (1993). *Wetlands in danger*. London, UK: Reed International Books.

Durieux, L., Kropacek, J., de Grandi, G., & Achard, F. (2007). Object-oriented and textural image classification of the Siberia GBFM radar mosaic combined with MERIS imagery for continental scale land cover mapping. *International Journal of Remote Sensing, 28*, 4175-4182

Farr, T.G., & Kobrick, M. (2000). Shuttle radar topography mission produces a wealth of data. American Geophysical Union, *Eos, 81*, 583-585

Forsberg, B., Araujo-Lima, C., Martinelli, L., Victoria, R., & Bonassi, J. (1993). Autotrophic carbon sources for fish of the central Amazon. *Ecology, 74*, 643-652

Gutjahr, E. (2000). Prospects for arable farming in the floodplains of the central Amazon. In W. J. Junk, J. J. Ohly, M. T.F. Piedade, & M. G. M. Soares (Eds.), *The Central Amazon floodplain: Actual use and options for a sustainable management* (pp. 141-170). Leiden: Backhuys Publishers.

Hamilton, S., Kellndorfer, J., Lehner, B., & Tobler, M. (2007). Remote sensing of floodplain geomorphology as a surrogate for biodiversity in a tropical river system (Madre de Dios, Peru). *Geomorphology, 89*, 23-38

Hart, T., & Hart, J. (1986). The ecological basis of hunter-gatherer subsistence in African rain forests: the Mbuti of eastern Zaire. *Human Ecology, 14*, 29-55

Hess, L., Melack, J., Filoso, S., & Wang, Y. (1995). Delineation of inundated area and vegetation along the Amazonfloodplain with the SIR-C synthetic aperture radar. *IEEE Transactions on Geoscience and Remote Sensing, 33*, 896-904

Hess, L., Melack, J., Novo, E., Barbosa, C., & Gastil, M. (2003). Dual-season mapping of wetland inundation and vegetation for the central Amazon basin. *Remote Sensing of Environment, 87*, 404-428

Houhoulis, P. F., & Michener, W. K. (2000). Detecting wetland change: a rule-based approach using NWI and SPOT-XS data. *Photogrammetric Engineering and Remote Sensing, 66*, 205-211

Hughes, R. H., Hughes, J. S., & Bernacsek, G. (Eds.) (1992). *A directory of African wetlands*. Cambridge: IUCN/UNEP/WCMC.

International Rivers (2008). Grand Inga Dam, D.R. Congo. Online at: http://internationalrivers.org/en/node/345

Junk, W. J. (Ed.) (1997). The Central Amazon Floodplain: Ecology of a Pulsing System*. Ecological Studies, Vol. 126.* New York, NY: Springer-Verlag.

Junk, W., Bayley, P., & Sparks, R. (1989). The flood pulse concept in river–floodplain systems. Proceedings of the International Large River Symposium, *Canadian Special Publication of Fisheries and Aquatic Sciences, 106*, 110-127.

Junk, W. (2002). Long-term environmental trends and the future of tropical wetlands. *Environmental Conservation, 29*, 414-435

Keddy, P., Fraser, L., Solomeshch, A., Junk, W., Campbell, D., Arroyo, M., & Alho, C. (2009). Wet and Wonderful: The World's Largest Wetlands Are Conservation Priorities. *BioScience, 59*, 39-51

Landis, J., & Koch, G. (1977). The measurement of observer agreement for categorical data. *Biometrics, 33*, 159-174

Laporte, N., Goetz, S., Justice, C., & Heinicke, M. (1998). A new land cover map of central Africa derived from multi-resolution, multi-temporal AVHRR data. *International Journal of Remote Sensing, 19*, 3537-3550

Lehner, B., & Döll, P. (2004). Development and validation of a global database of lakes, reservoirs and wetlands. *Journal of Hydrology, 296*, 1-22

Lehner, B., Verdin, K., & Jarvis, A. (2006). *HydroSHEDS Technical Documentation.* World Wildlife Fund US, Washington, DC.

Leroux, M. (1983). *Le climat de l'Afrique tropicale*. Editions Champion, Paris.

Lobo, A. (1997). Image segmentation and discriminant analysis for the identification of land cover units in ecology. *IEEE Transactions on Geoscience and Remote Sensing, 35*, 1136-1145

Mayaux, P., Richards, T., & Janodet, E. (1999). Special Paper: A Vegetation Map of Central Africa Derived from Satellite Imagery. *Journal of Biogeography*, 353-366

Mayaux, P., De Grandi, G., & Malingreau, J. (2000). Central African forest cover revisited - A multisatellite analysis. *Remote Sensing of Environment, 71*, 183-196

Mayaux, P., De Grandi, G., Rauste, Y., Simard, M., & Saatchi, S. (2002). Large-scale vegetation maps derived from the combined L-band GRFM and C-band CAMP wide area radar mosaics of Central Africa. *International Journal of Remote Sensing, 23*, 1261-1282

Mayaux, P., Bartholomé, E., Fritz, S., & Belward, A. (2004). A new land-cover map of Africa for the year 2000. *Journal of Biogeography (J. Biogeogr.), 31*, 861-877

Melack, J.M. & Forsberg, B.R. (2001) Biogeochemistry of Amazon floodplain lakes and associated wetlands. In M. E. McClain, R. L. Victoria & J. E. Richey (Eds.), *The biogeochemistry of the Amazon basin and its role in a changing world* (pp. 235-274). Oxford, UK: Oxford University Press.

Melack, J. M., Hess, L. L., Gastil, M., Forsberg, B. R., Hamilton, S. K., Lima, I. B. T., & Novo, E. M. L. M. (2004). Regionalization of methane emissions in the Amazon Basin with microwave remote sensing. *Global Change Biology, 10*, 530-544

Mertes, L. (2002). Remote sensing of riverine landscapes. *Freshwater Biology, 47*, 799-816

Oliver, C., & Quegan, S. (1998). Understanding synthetic aperture radar images. Raleigh, NC: Scitech Publishing.

Ozesmi, S., & Bauer, M. (2002). Satellite remote sensing of wetlands. *Wetlands Ecology and Management, 10*, 381-402

Pontius, R. (2000). Quantification error versus location error in comparison of categorical maps. *Photogrammetric Engineering and Remote Sensing, 66*, 1011-1016

Richey, J., Melack, J., Aufdenkampe, A., Ballester, V., & Hess, L. (2002). Outgassing from Amazonian rivers and wetlands as a large tropical source of atmospheric CO2. *Nature, 416*, 617-620

Rosenqvist, Å., & Birkett, C. (2002). Evaluation of JERS-1 SAR mosaics for hydrological applications in the Congo river basin. *International Journal of Remote Sensing, 23*, 1283-1302

Rosenqvist, Å., Forsberg, B., Pimentel, T., Rauste, Y., & Richey, J. (2002). The use of spaceborne radar data to model inundation patterns and trace gas emissions in the central Amazon floodplain. *International Journal of Remote Sensing, 23*, 1303-1328

Rosenqvist, A., Finlayson, C., Lowry, J., & Taylor, D. (2007). The potential of long-wavelength satellite-borne radar to support implementation of the Ramsar Wetlands Convention. *Aquatic Conservation: Marine and Freshwater Ecosystems, 17*

Runge, J., & Nguimalet, C. (2005). Physiogeographic features of the Oubangui catchment and environmental trends reflected in discharge and floods at Bangui 1911–1999, Central African Republic. *Geomorphology, 70*, 311-324

Runge, J. (2007). The Congo River, central Africa. In Gupta, A. (Ed.) *Large Rivers: Geomorphology and Management,* (pp. 294-309). New York: John Wiley & Sons, Ltd.

Sader, S., Ahl, D., & Liou, W. (1995). Accuracy of Landsat-TM and GIS rule-based methods for forest wetland classification in Maine. *Remote Sensing of Environment, 53*, 133-144

Sahagian, D., & Melack, J. (1998). Global wetland distribution and functional characterization: Trace gases and the hydrologic cycle. Report from the joint GAIM/IGBP-DIS/IGAC/LUCC workshop. IGBP Report No. 46, IGBP Secretariat, Stockholm.

Semeniuk, V., & Semeniuk, C. (1997). A geomorphic approach to global classification for natural inland wetlands and rationalization of the system used by the Ramsar Convention–a discussion. *Wetlands Ecology and Management, 5*, 145-158

Silva, T., Costa, M., Melack, J., & Novo, E. (2008). Remote sensing of aquatic vegetation: theory and applications. *Environmental Monitoring and Assessment, 140*, 131-145

Simard, M., De Grandi, G., Saatchi, S., & Mayaux, P. (2002). Mapping tropical coastal vegetation using JERS-1 and ERS-1 radar data with a decision tree classifier. *International Journal of Remote Sensing, 23*, 1461-1474

SPIAF (1995). Carte forestiere de synthese de la Republique Democratique du Congo, Service Permanent d'Inventaire et d'Amenagement Forestier, Kinshasa

Sterling, S., & Ducharne, A. (2008). Comprehensive data set of global land cover change for land surface model applications. *Global Biogeochemical Cycles, 22*

Thieme, M., Lehner, B., Abell, R., Hamilton, S., Kellndorfer, J., Powell, G., & Riveros, J. (2007). Freshwater conservation planning in data-poor areas: an example from a remote Amazonian basin (Madre de Dios River, Peru and Bolivia). *Biological Conservation, 135*, 484-501

United Nations (2000). World population prospects: the 2000 revision. Online at http://www.un.org/esa/population/publications/wpp2000/wpp2000h.pdf

Vancutsem, C., Pekel, J., Evrard, C., Malaisse, F., & Defourny, P. (2009). Mapping and characterizing the vegetation types of the Democratic Republic of Congo using SPOT VEGETATION time series. *International Journal of Applied Earth Observations and Geoinformation, 11*, 62-76

Welcomme, R. (1979). Fisheries ecology of floodplain rivers. London: Longman.

White, F. (1983). The vegetation of Africa: a descriptive memoir to accompany the UNESCO/AETFAT/UNSO vegetation map of Africa. *Natural Resources Research, 20*, 1–356